THE PENNSYLVANIA STATE UNIVERSITY

SCHREYER HONORS COLLEGE

DEPARTMENT OF BIOCHEMISTRY AND MOLECULAR BIOLOGY

CHARACTERIZATION OF TUDOR STAPHYLOCOCCAL NUCLEASE IN PLASMODIUM YOELII

OLIVIA SMITH

SPRING 2020

A thesis
submitted in partial fulfillment
of the requirements
for a baccalaureate degree in
Microbiology
with honors in Microbiology

Reviewed and approved* by the following:

Scott Lindner
Assistant Professor of Biochemistry and Molecular Biology
Thesis Supervisor

Paul Babitzke
Professor of Biochemistry and Molecular Biology
Honors Adviser

Wendy Hanna-Rose
Professor of Biochemistry and Molecular Biology
Department Head

*Signatures are on file in the Schreyer Honors College

Abstract

Plasmodium parasites are the causative agent of malaria, a disease which afflicted an estimated 219 million people in 2017. The life cycle of these parasites depends on the ability to transmit to mosquitoes, which can then re-infect a host; as such, transmission is a highly regulated process. Through use of *Plasmodium yoelii,* a strain of the parasite which infects rodents, we are investigating the role of a highly conserved tudor staphylococcal nuclease (TSN) in the transmission process. In other organisms, TSNs are involved in gene expression, but in *P. yoelii*, the function of PyTSN1 is not well understood. Our lab has previously demonstrated that PyTSN1 interacts with translational repressors ALBA4 and CITH, and the CAF1/CCR4/NOT complex, all of which are involved in transmission of malaria parasites to mosquitoes.

To better characterize this protein, I have generated three transgenic parasite lines to identify the function, localization, and protein-protein interactions of PyTSN1 through gene deletion, fluorescent tagging, and proteomics approaches, respectively. Immunofluorescence assays suggest that PyTSN1 is primarily located in the cytoplasm of asexual blood stage parasites and gametocytes. Additionally, PyTSN1 appears to colocalize with CITH, a translational repressor found abundantly in female gametocytes. Protein-protein interactions were determined through the use of a proximity labelling system in which biotin is used as a tag to mark proximal proteins to PyTSN1. Finally, the *pytsn1*$^{-}$ transgenic parasite line is being analyzed in order to determine if the lack of PyTSN1 conveys any sort of defect in the parasite life cycle. The ultimate goal of this project is to better understand the localization, function, and interactions of PyTSN1 in order to better understand the role this protein plays in transmission of the parasite.

TABLE OF CONTENTS

LIST OF FIGURES

LIST OF TABLES

Acknowledgements

I would like to thank my thesis supervisor Dr. Scott Lindner for all that he has done to support me as a student and a scientist. His mentorship has been invaluable to me for the last two and a half years, and I am grateful for the guidance he has provided, both during the completion of this thesis and during my applications to graduate school. In addition, I would like to thank graduate student Kelly Rios for her patience and guidance throughout this project. Thank you, too, to the members of the Lindner Laboratory for always being willing to share their expertise. The staff at the vivarium, who cared for the mice during the course of this project, were also essential to seeing its completion. Finally, I would like to recognize the sources that provided funding for these experiments, including the start-up funds given to Scott Lindner by The Pennsylvania State University and the undergraduate research grants from the Eberly College of Science.

Chapter 1

Introduction

Plasmodium parasites are the causative agents of malaria, a disease which afflicted an estimated 228 million people, which included 405,000 deaths, in 2018[25]. Among those most susceptible to the disease are young children and pregnant women, who have a higher likelihood of developing symptoms of severe illness including severe malarial anemia and cerebral malaria[22] As these eukaryotic parasites rapidly develop drug resistance to available antimalarials and the sole licensed vaccine has limited efficacy, the biology of *Plasmodium* parasites must be further researched in order to support drug and vaccine development.

Plasmodium spp., like many parasites, have a complex life cycle in which the parasite moves between vertebrate host and mosquito vector[4.] The life cycle begins when an infected mosquito bites a host, facilitating the transmission of sporozoites from the mosquito salivary gland skin, from which they migrate into the bloodstream. These parasites then travel to the liver, where they invade hepatocytes and develop into merozoites of several days. The hepatocyte, containing as many as 40,000 parasites, bursts, releasing bundles of merozoites (merosomes) into the bloodstream. Merozoites in the blood invade erythrocytes by interacting with the surface of a cell then actively entering the cell by forming a vacuole derived from the plasma membrane. Inside the parasitophorous vacuole, the parasite begins its asexual blood stage replication first as a ring, then as a trophozoite, and finally amplify their numbers through schizogony as schizonts. Developed schizonts lyse the cell, releasing merozoites that continue the asexual intraerythrocytic developmental cycle. In some instances, the parasite instead differentiates into either a male or female gametocyte. These gametocytes mature and circulate in the blood,

waiting to be taken up by a mosquito during a blood meal. Once inside the midgut of the mosquito, male and female gametocytes undergo gametogenesis to form male and female games, which can fuse to form a zygote. The zygote develops into a motile ookinete, which can move through the midgut wall and form an oocyst on the surface of the midgut. Inside of the oocyst, the parasite replicates; eventually the oocyst bursts and sporozoites emerge to begin migration through the hemocoel to bind to and invade the salivary gland of the mosquito. In the salivary gland, the sporozoites wait in anticipation of another bite and a new host. This life cycle facilitates the infection of many hosts (Figure 1.1) [4] .

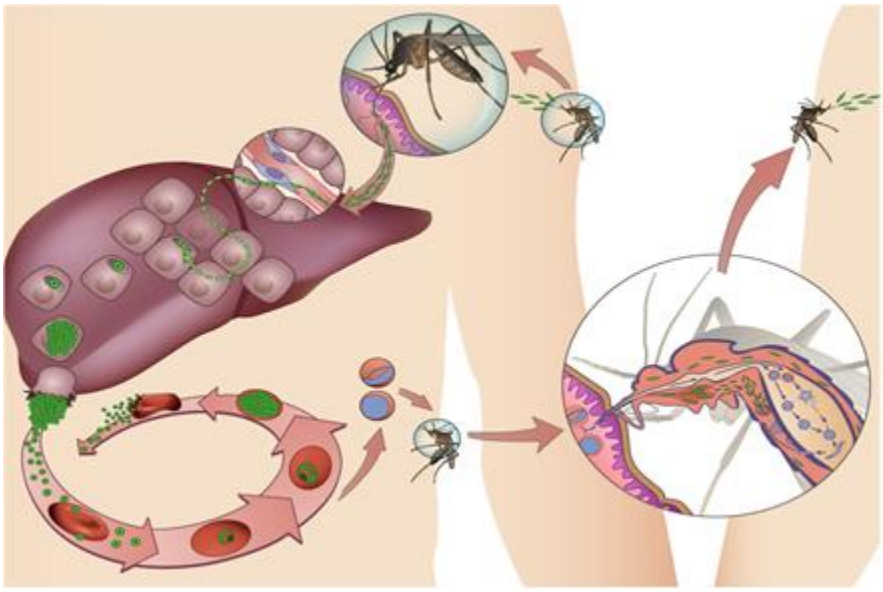

Figure 1.1

Figure 1.1: A schematic of the Plasmodium spp. lifecycle showing parasites moving between mosquito host and vertebrate vector. Image courtesy of Maria Mota, Instituto de Medicina Molecular, Lisbon, Portugal.

The stages in which a parasite moves from mosquito to human as sporozoites and from human to mosquito as gametocytes are transmission stages. Transmission stage biology has not yet been fully elucidated, but translational repression is known to play a significant role in the

development of transmission stages and progression through the life cycle. Post-transcriptional gene regulation is used by *Plasmodium spp.* to prepare for a transmission event and then rapidly react to a new environment upon transmission by translating previously transcribed mRNAs. Two basic strategies the parasite uses to moderate availability of transcripts have been outlined: repression of targeted mRNAs and global repression of translation. Sporozoites, for example, exhibit global repression of transcription in preparation for a mosquito bite; this is facilitated by the phosphorylation state of a translation initiation factor. Upon transmission from mosquito to human tissue, the repression is relieved and translation occurs, as reviewed in Rios and Lindner.

Alternatively, targeted mRNAs are repressed in female gametocytes in preparation for zygote formation and development. This strategy is used by *Plasmodium spp.* as well as other eukaryotic organisms prior to formation of a zygote[12]. Generally, multicellular organisms can silence transcripts by sequestering them in a complex akin to a germ granule or a P granule in *Caenorhabditis elegans*, inside of a female gamete. These granules then dissolve upon fertilization to facilitate translation and transition from gamete to zygote[21]. Similarly, female gametocytes depend on the silencing of certain genes in granular structures until transmission occurs. These ribonucleoprotein (mRNP) particles are necessary to prepare the parasite to change in reaction to the hostile environment that is the mosquito midgut and facilitate rapid development post-fertilization[13] .Stability of these mRNPs depends on an DEAD-box RNA helicase, DOZI (orthologue of human DDX6 and yeast Dhh1); without DOZI, these complexes dissolve and transcripts intended to be preserved are degraded, as has been shown in *Plasmodium berghei*[12]. An additional critical protein in this process is CITH (orthologue of LSM14A), which its gene is deleted results in female gametocytes that cannot contribute to ookinete formation. *pbdozi-/ pbcith-* parasites are capable of forming zygotes, but the repressed

transcripts are not available to facilitate appropriate development of ookinetes[13]. A variety of other proteins are found in these complexes, including proteins of the nucleic acid-binding ALBA family[17] In order for female gametocytes to contribute transcripts necessary for ookinete formation, CITH and DOZI must be present to mediate mRNA silencing.

Comparative analysis of transcriptomic and proteomic data can elucidate which transcripts are being repressed and has been applied to female gametocytes. In *Plasmodium falciparum*, 512 transcripts were detected without a corresponding protein, including transcripts used to facilitate ookinete formation and maturation. Among these transcripts are those for *p28*, which encodes an ookinete surface protein functioning as an adhesin and *pfap2-o*, which yields a specific transcription factor vital for *Plasmodium* infection of mosquitoes. Additionally, mRNAs that encode for proteins found in the DOZI/CITH complex are more abundant in female gametocytes in comparison to other blood stage parasites[16]. Similar work in *P. berghei* identified 731 mRNA transcripts that were associated with the DOZI/CITH complex, and thus may be repressed. These transcripts were identified, and included again p28 and similar adhesin p25, transcription factor *ap2-o*, and a wide variety of transcripts coding for ookinete-specific proteins. These ookinete proteins coded for by repressed transcripts included those for motility proteins (CTRP), midgut recognition (WASPs, SOAPs, PSOPs), midgut invasion (PPLP3), cell traversal (CelTOS), 40 proteins involved in gliding motility, and several unidentified proteases[7]. Disruption of translational repression mechanisms and inhibition of translation in zygotes have the same phenotype: no ookinetes can form in the mosquito midgut. The severe phenotype is not present if transcription is inhibited in zygotes, implying that the critical step is translation of repressed transcripts, not transcription and translation of new genes[7]. Female gametocyte translational repression, dependent on proteins CITH and DOZI, is required for ookinete

formation and maturation. However, male gametocytes and asexual blood stage parasites utilize other methods to moderate their mRNA.

Our lab has previously characterized two proteins, that are important for mRNA regulation in *Plasmodium yoelii* blood stage parasites: PyCCR4-1 and PyALBA4. CCR4-1 is a putative deadenylase that associates with CAF1 and NOT in a complex that is conserved throughout essentially all eukaryotes. The CAF1/CCR4/NOT protein complex has a wide variety of functions, from regulating transcription and mRNA export from the nucleus to moderating translatability of mRNA and degrading mRNAs in the cytoplasm[26]. In *Plasmodium* spp. and other eukaryotes it can be found in cytoplasmic granule structures. Male *Plasmodium yoelii* parasites lacking this protein have dysregulated maturation impairing exflagellation, the process by which male gametes release into the environment in order to facilitate fertilization of female gametes and formation of a zygote. Dysregulated exflagellation hinders transmission from host to mosquito. Investigation of the specific functionality of CCR4-1 indicates that the protein is not solely acting as a deadenylase as there are no discrepancies in the UTR composition of poly-A tail of affected transcripts that were studied[10].

ALBA4 is another critical protein used by both blood stage asexual parasites and gametocytes to moderate gene expression. Generally, the role of ALBA4 in a parasite depends on the stage the parasite is in. In asexual blood stage parasites, where it localizes to cytosolic puncta, ALBA4 is involved in normal mRNA turnover, while in gametocytes it protects normal gene expression in *Plasmodium yoelii*[15]. Asexual blood stage parasites lacking PyALBA4 through gene deletion show no significant phenotype. However, *pyalba4-* male gametocytes exhibit an increase in the activation of gametocytes, indicating it acts as a repressor of exflagellation gene expression in wild-type parasites, either directly or indirectly. PyALBA4 also

plays a critical role in the semi-synchronous egress of oocyst sporozoites from the oocyst. While in wild type parasites egress and movement to the salivary glands typically occurs in a short period of time, parasites lacking PyALBA4 cannot tightly coordinate their egress and/or invasion of the salivary gland[15].

Both Hart *et al* 2019 and Munoz *et al* 2017 did proteomics studies of interacting proteins of CCR4-1 and ALBA4 respectively by crosslinking immunoprecipitation and tandem mass spectrometry in *Plasmodium yoelii*. These crosslinking experiments identified numerous proteins affiliated with the targeted regulatory proteins. Among the proteins identified as interacting with both CCR4-1 and ALBA4 is a protein previously uncharacterized in *Plasmodium yoelii:* Tudor Staphylococcal Nuclease 1 (PyTSN1 PlasmoDB GeneID: PY17XNL_0913800).

PyTSN1 is a member of the broad family of Tudor Staphylococcal Nucleases, which are linked by their structure and their multifunctional activity. TSN family proteins, composed of five staphylococcal nuclease domains and one Tudor domain, are evolutionarily conserved across all domains of life. TSN family proteins have been shown to act as scaffolds for protein-protein interactions and nucleases; these functions are useful in regulating gene expression, which is the role many TSN proteins play in organisms. Additionally, cleavage of the TSN family protein p100 is one of the steps in facilitating cell death by apoptosis[8]. With a wide variety of roles for TSN family proteins, examination of the role of TSN proteins in protozoa is useful to begin understanding what TSN1's role may be in *Plasmodium yoelii.*

In *Entamoeba histolytica,* TSN family proteins have been shown to act as transcription factors, binding upstream regulatory elements. EhTSN has been shown to localize in the nucleus with euchromatin but not heterochromatin, implying it would be related to transcription. It has also been shown to interact with URE1, a cis-regulatory element that moderates the transcription

of virulence genes[3]. EhTSN has also been linked to vesicle membranes and the plasma membrane where the protein appears to be interacting with transcripts, controlling metabolic processes, and facilitating cellular signaling. EhTSN has also been shown to colocalize with HSP70 during heat shock, thus implicating it in stress response as well. In *E. histolytica,* TSN has been shown to localize to the nucleus and the cytoplasm, depending on its function[3].

In *Plasmodium falciparum,* work has been done to examine PfTSN localization and function. PyTSN1 and PfTSN are orthologous. PfTSN localizes primarily in the nucleus in asexual blood stage parasites[11] and appears to be involved in ensuring the preservation of specific mRNAs. PfTSN may be essential in asexual blood stage parasites, as inhibition of the protein can arrest development[23]. It may also be that PfTSN is actively using its nuclease domains, as micrococcal nuclease inhibitors produce the same stunted development, however these micrococcal nuclease inhibitors may have also been affecting other proteins that could cause this phenotype[11,23].

PyTSN1's presence in post-transcriptional regulatory complexes with CCR4-1 and ALBA4 indicate that PyTSN1 itself may play a role in mRNA modulation during the *P. yoelii* life cycle, including during development of transmission stages. The purpose of this study was to further elucidate the functionality of PyTSN1 inside *P. yoelii* by examining the localization patterns of PyTSN1 in various stages of the parasite lifecycle, estimating protein-protein interactions through use of a proximity-based labelling system, and observing any phenotypes associated with deletion of *pytsn1*.

Chapter 2
Materials and Methods

Experimental Animals

The mice utilized were all six- to eight- week old Swiss Webster female mice from Envigo. Mosquitoes used were *Anopheles stephensi* originally obtained from the Center for Infectious Disease Research in Seattle, WA and reared in the Lindner Lab. Mosquitoes were reared at 24 C and 70% humidity and were used to examine the *Plasmodium yoelii* parasite lifecycle. The Pennsylvania State University Institutional Animal Care and Use Committee (IACUC # 42678) approved all experiments performed, and each experiment followed the Association for Assessment and Accreditation of Laboratory Animal Care (AAALAC) guidelines.

Generation of Transgenic Parasite Lines

Plasmid Generation

Generation of three parasite lines necessitated production of three plasmids and their subsequent transfection into the Py17XNL strain of *Plasmodium yoelii*. The three transgenic lines made in order to conduct the major experiments included a genetic deletion, *pytsn1⁻;* a C-terminal GFP-tagged line, PyTSN1::GFP; and a line for proximity labelling, PyTSN1::TurboID::GFP. Targeting sequences for each vector were generated using sequence overlap extension (SOE) PCR. Primers (Appendix) were used to amplify the TSN1 targeting regions (including the 3’ UTR, CDS, and 5’ UTR) from genomic DNA (PY17XNL strain) with Phusion polymerase (NEB). SOE PCR was conducted to fuse a portion of the 3’ UTR with the 3’ end of the coding sequence (CDS), with the purpose of generating a C-terminally tagged

PyTSN1. Similarly, the 3' UTR and 5' UTR were fused by SOE PCR, with the purpose of generating a gene deletion. All nucleic acid products were purified on an agarose gel (1%), gel extracted (QIAquick Gel Extraction Kit, Qiagen, Cat#28706), ethanol precipitated, and quantified using a NanoDrop ™ 2000 spectrophotometer. They were then ligated into a pCR-Blunt intermediate vector expressing a Ampicillin resistance gene for selection. Restriction digests were used to confirm the plasmid's size, and Sanger Sequencing (Penn State Sequencing Core) confirmed the sequences. The target nucleic acids were cut from pCR-Blunt using restriction enzymes KpnI and SpeI and ligated into a terminal vector. Final vectors used included 1) a vector for gene deletions that contains a Green Fluorescence Protein mutant 2 (GFPmut2) cassette for visualization and a human dihydrofolate reductase (HsDHFR) cassette for drug selection, 2) a vector containing a TurboID tag fused with a, a GFPmut2 tag, and a separate HsDHFR cassette, 3) and an additional vector with a GFPmut2 tag and HsDHFR cassette. This strategy generated plasmids containing targeting regions that would facilitate development of transgenic parasite lines post-transfection (*pytsn1*$^{-}$, PyTSN1::TurboID::GFP, and PyTSN1::GFP, respectively. The plasmid DNAs were extracted and purified from *E. coli* using a Qiagen Plasmid Maxiprep Kit to prepare it for transfection.

Transfection and Growth of Parasites.

Transfection of the plasmid construct into Py17XNL strain parasites was facilitated by an overnight schizont preparation. Mice infected with Py17XNL were exsanguinated by cardiac puncture when parasitemia reached 1%. The parasites were synchronized to schizonts over 12 hours in complete RPMI (containing incomplete RPMI (Cellgro), 20% v/v Fetal Bovine Serum (Gibco), and Gentamycin (Invitrogen)) and gassed with 85% N_2, 5% CO_2, and 10% O_2. Schizonts were purified by discontinuous Accudenz gradient (working solution of 40%

commercial PBS without Ca or Mg and a 60% Accudenz stock, consisting of 27.6% Accudenz (Accurate Chemical and Scientific Corporation) in 100mL 5mM Tris pH7.5, 3 mM KCl, and 0.3 mM EDTA). The Accudenz gradient was centrifuged for 20 minutes at 200 *xg* and parasites were collected from the interface of the gradient. These parasites were pelleted by centrifuging at 200 *xg* for 10 minutes. The transfection was conducted using an Amaxa electroporator and Amaxa cuvettes; five to ten micrograms of ApaI and NheI -linearized plasmid were mixed with cytomix (120 mM KCl, 0.15 mM $CaCl_2$, 2 mM EDTA, 5 mM $MgCl_2$, 8.66 mM K_2HPO_4 pH 7.6, 1.34 mM KH_2PO_4 pH 7.6, and 25 mM HEPES pH7.6) in preparation for electroporation. Approximately 10 uL purified schizonts were added to the cytomix and plasmid solution. Electroporation was completed with program T-016. After electroporation, complete RPMI was added and the mixture was used to complete a tail vein injection into a Swiss Webster mouse, and was repeated as a technical duplicate.

Post-transfection, mice were put on pyrimethamine (0.007% w/v Fisher Scientific, Cat #ICN19418025) one day post transfection and were treated for three days. When parasitemia reached ~1-3%, the parental mouse was euthanized, and its blood collected for infecting a naïve mouse (transfer mouse) by IP injection and for storage in cryovials in liquid nitrogen. Genotyping PCR was done to determine if the plasmid integrated as designed into the parasite genome, and to assess the ratio of wild-type and transgenic parasites present in the population.

Fluorescence-Activated Cell Sorting (FACS)

Parasite lines expressing GFP in the asexual blood stage were selected for by GFP fluorescence using Fluorescence-Activated Cell Sorting (FACS) to enrich transgenic parasites in mixed populations. A new mouse was infected from the cryopreserved blood from the transfer mouse, and its parasitemia was allowed to grow to 1%. At that time, a schizont preparation was

done as previously described, collecting the parasites from the mouse to be filtered. The filtered parasites were run on the Beckman Coulter MoFlo Astrios EQ Cell Sorter (Penn State Flow Cytometry Facility) to sort out 20,000 GFP positive cells. These cells were collected in iRPMI and used to infect naïve mice by tail-vein injection. The newly-infected mice were monitored until parasitemia reached 1%, at which point they were euthanized and the parasite population was again cryopreserved and examined by genotyping PCR to determine if wild type parasites were present or if the population was entirely transgenic.

Limited Dilution Cloning

While non-clonal parasite populations were appropriate for studies of the parasite lines expressing TurboID::GFP -and GFP- tagged PyTSN1, characterization of the line with the genetic deletion of *pytsn1*$^{-}$ required clonal populations which were generated by limited dilution cloning. A mouse was infected with the mix of transgenic and wild type parasites produced from the transfer mouse during transfection, and it was monitored until parasitemia was 1-3%. The parasitemia was determined precisely by counting parasites smeared on a glass slide and stained by Giemsa. The mouse was euthanized and its blood harvested by cardiac puncture into incomplete RPMI. Blood in RPMI was serially diluted in RPMI to a final concentration of either 2.5 or 5 parasitized red blood cells per 100 uL of RPMI, determined by taking into account the precise parasitemia of the mouse. Each of the dilutions was used to infect 5 naïve mice. The Poisson distribution dictates that when ~37% of a group becomes positive, that those infections originated from one cell, thus generating a clonal parasite line. One mouse injected with the 2.5 parasitized RBC/ 100 uL RPMI dilution became infected, while two mice injected with the 5 parasitized RBC/ 100 uL RPMI dilution became infected. Mice that developed infections were euthanized and their blood harvested by cardiac puncture. Cryovials were made with the blood,

and the blood was used to run a genotyping PCR to confirm that the population was indeed solely transgenic parasites.

Blood Stage Immunofluorescence Assays

An indirect immunofluorescence assay (IFA) was conducted to determine the localization and timing of expression of PyTSN1::GFP within the parasite. Infected red blood cells were harvested from mice by a cardiac puncture. The cells were washed in 1x PBS and fixed in a mixture of 4% v/v para-formaldehyde, 0.015% v/v glutaraldehyde, in 1x PBS. They were then permeabilized with 0.1% v/v Triton X-100 in 1x PBS and blocked 3% w/v BSA. The cells were separated into three aliquots for visualization of separate stages of the parasite lifecycle present in the blood sample. An anti-GFP primary antibody was used to treat all cells in order to visualize PyTSN1::GFP. For two groups, those interrogating asexual parasites and female gametocytes, mouse monoclonal anti-GFP antibodies (clone 2F9) were used. For the male gametocytes, rabbit polyclonal anti-GFP antibodies were used. Counterstaining was done using three different primary antibodies for the three groups of cells: one group was treated with rabbit polyclonal anti-PyCITH antibodies to identify female gametocytes, another was treated with mouse monoclonal anti-α tubulin antibodies to identify male gametocytes, and the last was treated with rabbit polyclonal anti-PyACP antibodies to identify ring, trophozoite, and schizont stages of asexual blood stage parasites. All antibodies were 1:1000 dilutions in 3% w/v BSA. Cells were washed, and the fluorescent secondary antibodies were added. The two groups identifying asexual parasites and female gametocytes were treated with anti-rabbit IgG conjugated to AlexaFluor594 (red) and anti-mouse IgG conjugated to AlexaFluor488 (green)The group identifying male gametocytes was treated with anti-mouse IgG conjugated to AlexaFluor594 (red) and anti-rabbit IgG conjugated to AlexaFluor488 (green). Cells were again

washed, and a 1 ug/mL DAPI (4',6-diamidino-2-phenylindole) nucleic acid stain in 1x PBS was applied in the dark for 5 minutes. Cells were washed, placed on a slide and treated with an anti-fade reagent. Cells were then visualized using a Zeiss AxioScope A1 Fluorescent Microscope.

Proximity-Based Labelling with TurboID

In order to determine protein-protein interactions, a proximity-based labelling system was used, as described in Figure 3.15. TurboID, a modified *E.coli* BirA biotin ligase, was used in lieu of BioID due to its increased labelling efficiency over shorter periods of time (Branon et al). Appropriate experimental conditions were empirically determined as follows.

A schizont preparation was done as described above and was separated into six flasks. Exogenous biotin (150 mM final concentration) was added to determine the best duration of labeling. The longest time point was 12 hours incubation, with biotin added immediately after gassing the parasites with the same gas mixture used above. The next time point was 4 hours incubation with biotin (biotin was added at 8 hours post-gassing). Then 2 hours, 1 hour, 15 minutes, and finally no exogenous biotin added, thus ensuring that all cultures were grown for the same amount of time and harvested simultaneously. Each of these time points were then analyzed using a "pseudo-western blot", by probing with streptavidin-HRP to visualize proteins bound to biotin.

Schizonts for conducting an experiment were prepared in this way, with 4 hours incubation with 150 uM exogenous biotin. A discontinuous Accudenz gradient (as described above) was used for purification; parasites at the interface were collected and pelleted. Gametocytes were prepared for an experiment in a similar way. Naïve mice were infected from cryovials, and parasitemia was allowed to increase to 1%. At this point, the mice were treated

with medicated drinking water containing 10 mg/L sulfadiazine for two days, which kills asexual blood stage parasites but not gametocytes. Blood was collected by cardiac puncture into pre-warmed complete RPMI (37 C) and 150 uM biotin, gassed, and then the mixture was shaken at 37 C for 4 hours. Gametocytes were purified by Accudenz pre-warmed to 37 C to limit gametocyte activation into gametes. Parasites were collected from the interface and pelleted.

The parasite pellet was resuspended in a modified RIPA Lysis Buffer containing less SDS (50 mM Tris-HCl pH8, 0.1% w/v SDS, 1mM EDTA 150 mM NaCl, 1% w/v NP40, 0.5% w/v sodium deoxycholate, SUPERnase inhibitor, and 30% of a Roche Complete protease inhibitor tablet). DynaBeads MyOne Streptavidin T1 (Life Technologies) were washed twice with a filter sterilized solution A (100 mM NaOH 50 mM NaCl) and twice with a filter sterilized solution B (100 mM NaCl). The lysate was homogenized and sonicated. The lysate was then incubated with the washed beads for three hours, then washed in a modified RIPA Wash Buffer (50 mM Tris-HCl pH 8.0, 1 mM EDTA, 150 mM NaCl, 1% w/v NP40, and 60% a protease inhibitor tablet). A quarter of the beads were treated with 2X sample buffer (50 mM Tris pH 6.8, 5% w/v SDS, 5% v/v glycerol, 0.16% w/v Bromophenol Blue), 5% v/v beta-mercaptoethanol, and 1 mM biotin to elute the proteins. A quality control experiment to ensure that biotinylated proteins had bound to the beads was conducted by a “pseudo-western blot” as described above was run with the input, flow through, and elution, and was probed with streptavidin-HRP. The remaining 75% of the beads were stored at -80 C and then sent to the Indiana Proteomics Core for tandem LC-MS/MS.

Analysis of Mass Spectrometry Data

Trans Proteomic Pipeline (TPP, Institute for Systems Biology, Seattle, WA) was used to analyze raw mass spectrometry data. Raw data files were converted to .mxML files using

MsConvert and uploaded into TPP. Spectra were compared against reference proteomes of *Plasmodium yoelii* 17XNL (originating from PlasmoDB), mice (originating from Uniprot), and a common repository of adventitious protein sequences (CRAPome). TPP was also used to generate randomized decoys. Peptides from the X!Tandem Search and Comet Search were identified and combined using ProteinProphet to infer the protein identities.

Mosquito Feeds

Blood containing parasites was stored in liquid nitrogen. This blood was used to infect mice intraperitoneally. Centers of movement (exflagellation by male gametes) in a monolayer of red blood cells were checked using a wet mount of blood from infected mice using a phase contrast microscope with a 40X objective. When exflagellation of male gametocytes reached its peak, typically around day 4 or day 5 post infection, the mice were prepared for feeding by injecting a 100 mg/kg ketamine and 10mg/kg xylazine mixture in 1xnPBS without calcium or magnesium. Two anesthetized mice containing *pytsn1*$^{-}$ parasites were fed to starved mosquitoes for 15 minutes. A control transgenic parasite line constitutively expressing GFP (Py489) from a dispensable genomic locus was also fed to mosquitoes. After seven days, mosquito midguts were dissected to determine the number of oocysts present. After fourteen days, salivary gland dissections were conducted and salivary gland sporozoites were counted using a Hausser Bright Line-Phase hemocytometer (Fisher Scientific, Cat #02-671-6).

Chapter 3
Results

Generation of Parasite Lines

Three transgenic parasite lines were generated through reverse genetics. Plasmids bearing targeting sequences generated by PCR using genomic DNA from *Plasmodium yoelii* 17XNL strain (Py17XNL) were used to replace portions of the *pytsn1* genomic locus and are depicted in Figures 3.1-3.3.

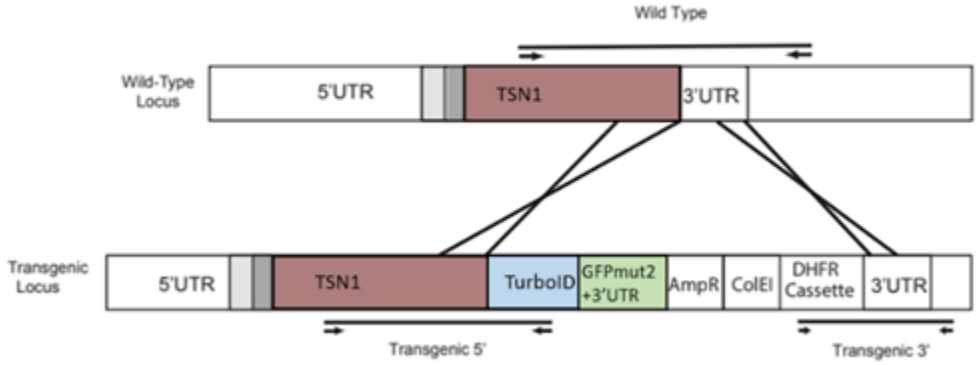

Figure 3.1

Figure 3.1: TurboID, GFPmut2, and a DHFR cassette were integrated into the *Plasmodium yoelii* genome during transfection of the final constructed plasmid. A schematic shows the recombination event during parasite transfection that facilitated integration of the transgenic plasmid into the Py17XNL genome. This was confirmed by genotyping PCR (Figure 3.8) and the presence of GFP signal. The location of the primers and the amplified regions by gPCR are labelled.

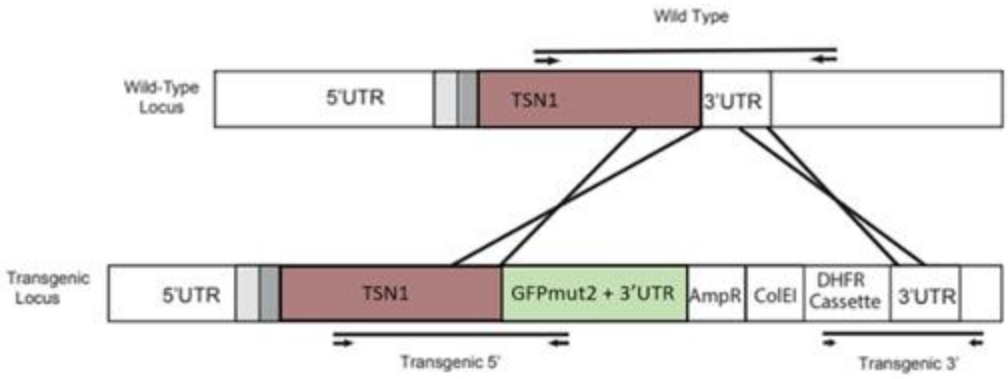

Figure 3.2

Figure 3.2: GFPmut2 and a DHFR cassette were integrated into the *P. yoelii* genome during transfection of the final constructed plasmid. A schematic shows the recombination event during transfection that facilitated integration of the transgenic locus into the Py17XNL genome. Integration was verified by genotyping PCR (Figure 3.8) and the presence of GFP signal. The location of gPCR primers and amplified regions are labelled.

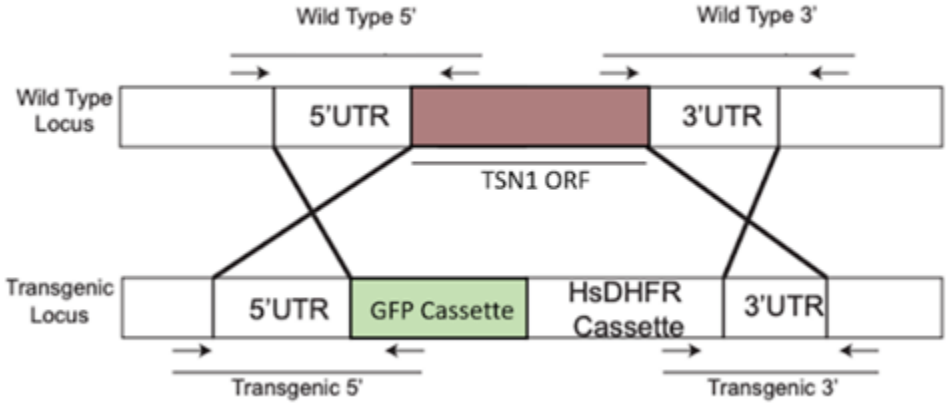

Figure 3.3

Figure 3.3: GFPmut2 and a DHFR cassette were integrated into the *P. yoelii* genome, replacing the *pytsn1* ORF, during a trasnfection using the final plasmid construct. A schematic shows the recombination event during transfection that facilitated integration of a transgenic locus in the genome of Py17XNL. Integration into the genome was verified by genotyping PCR (Figure 3.9) and the presence of GFP signal. The location of the primers and amplified regions during gPCR are labelled.

Portions of the 3’ UTR, CDS, and 5’ UTR of *pytsn1* were all PCR amplified (Figure 3.4) and fused by SOE PCR (Figure 3.5). Components of SOE PCR were amplified using appropriate primers (See Appendix) from wild type Py17XNL genomic DNA. As seen in Figure 3.4, the 3’ UTR and the coding sequence (CDS) targeting regions were successfully amplified but the 5’ UTR was not. The 5’ UTR ultimately was amplified using alternative primers by Dr. Kevin Hart in the Lindner Lab.

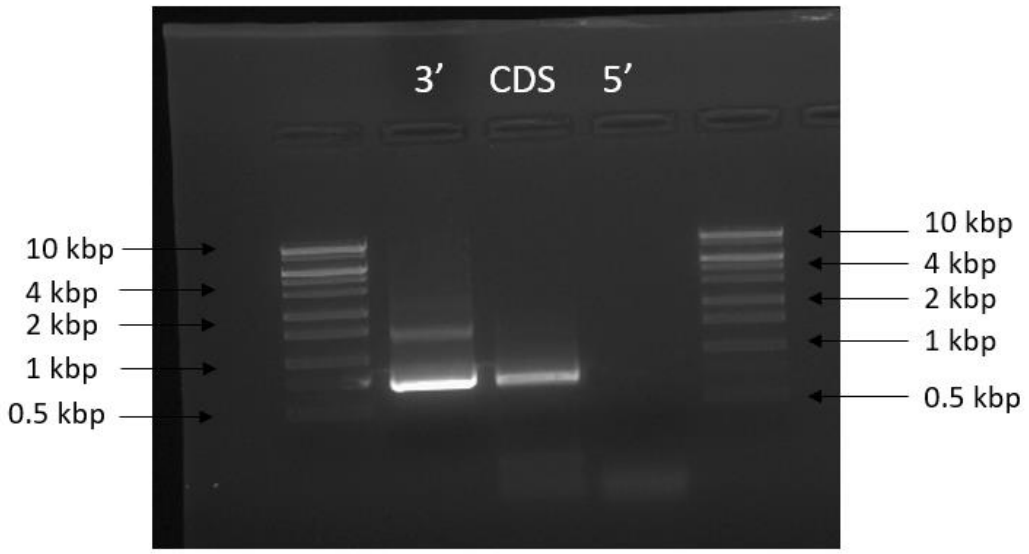

Figure 3.4

Figure 3.4: Gel image exhibiting amplification of targeting regions in *pytsn1*, specifically the 3’ UTR and the coding sequence (CDS).. Expected band sizes were 758 bp for the 3’ UTR region, 567 bp for the CDS region, and 727 bp for the 5’ UTR. While there was a major band in the 3’ UTR at the appropriate size, the band of amplified CDS region ran high and there was no band indicating amplification of 5’ UTR. Both the major 3’ UTR band and the CDS band were excised and extracted to be used in subsequent SOE PCRs.

The 3’ UTR and the 5’ UTR were combined via SOE PCR to facilitate generation of a gene deletion parasite line. The 3’ UTR and the CDS regions were combined in order to facilitate generation of a parasite line with a C-terminal tag on PyTSN1; one line was generated with a GFP tag and another was generated with both TurboID and GFP tags.

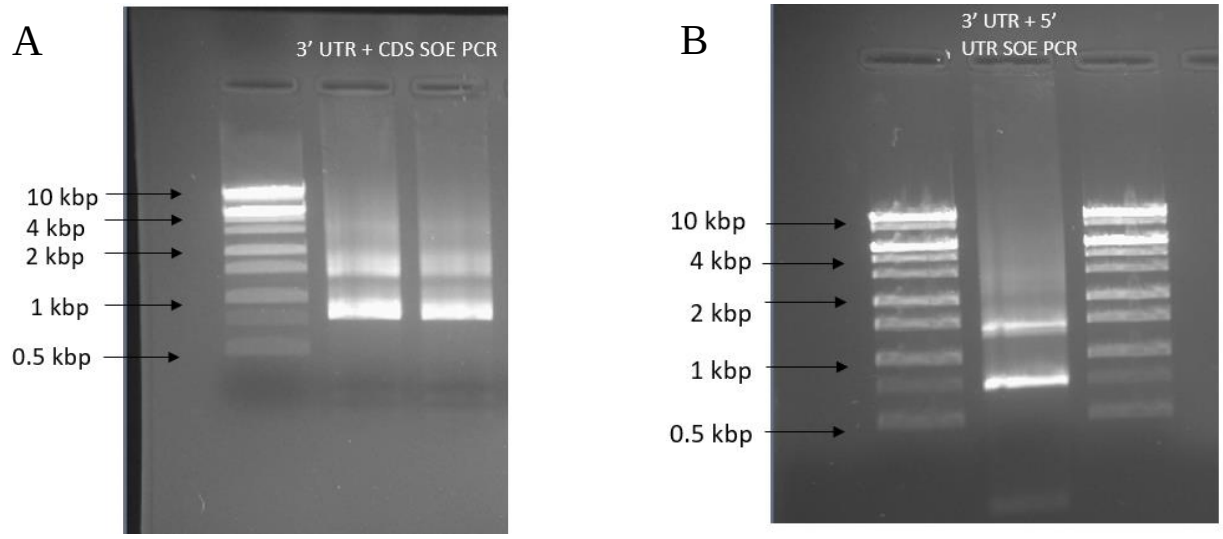

Figure 3.5

Figure 3.5: (A) *pytsn1* 3'UTR-CDS SOE PCR product was generated by SOE PCR. The expected band size was ~ 1500 bp. The major, lower band was the input PCR product that was not used in the reaction; the upper band was excised and extracted for ligation with pCR-Blunt pBS2254. (**B) The 3'UTR-5'UTR SOE PCR product was generated by SOE PCR.** The expected band size was ~1500 bp. The upper band was excised and extracted for ligation with pCR-Blunt pBS2254.

The SOE PCR product was then ligated into the StuI site of pCR-Blunt. The plasmid was transformed, grown in *Eschericia coli* with ampicillin selection, and colonies were screened for the presence of the inserted sequence by colony PCR (Figure 3.6). After transformation of the ligation product of PCR-Blunt pBS2254 and 3'-CDS SOE PCR product, the colony PCR screened for bacteria that had plasmids with an insertion of the SOE product into pCR-Blunt. Positive colonies were further screened by a diagnostic digest and Sanger sequencing to identify those with the correct sequence.

Figure 3.6

Figure 3.6: Colony PCR was conducted on *E. coli* to screen for bacteria that had plasmids with an insertion of the plasmid. Colonies were selected if they grew on LB+ Ampicillin plates, as the insert contained coding for ampicillin resistance. Out of 28 total colonies picked, two contained bands at an appropriate size to be considered positive (~2000 bp). These were colonies 13 and 18.

.

After determination that the SOE PCR product had be integrated into the intermediate vector pCR-Blunt, the plasmid was digested and the SOE PCR product ligated into the destination vector. The destination vector varied depending on the goal of the end plasmid. The 3' UTR + 5' UTR SOE product was ultimately integrated into a final plasmid (empty vector: pSL0444) that would facilitate replacement of the PyTSN1 ORF with one instead coding for GFP. The 3' UTR + CDS SOE PCR product was used for two final plasmids. The first was designed to add a C-terminal GFP tag to PyTSN1 (empty vector: pSL0442). The second was

designed to add a C-terminal TurboID and GFP tag to PyTSN1 (empty vector: pSL1360). Integration of the SOE product into the terminal vector was again analyzed by colony PCR.

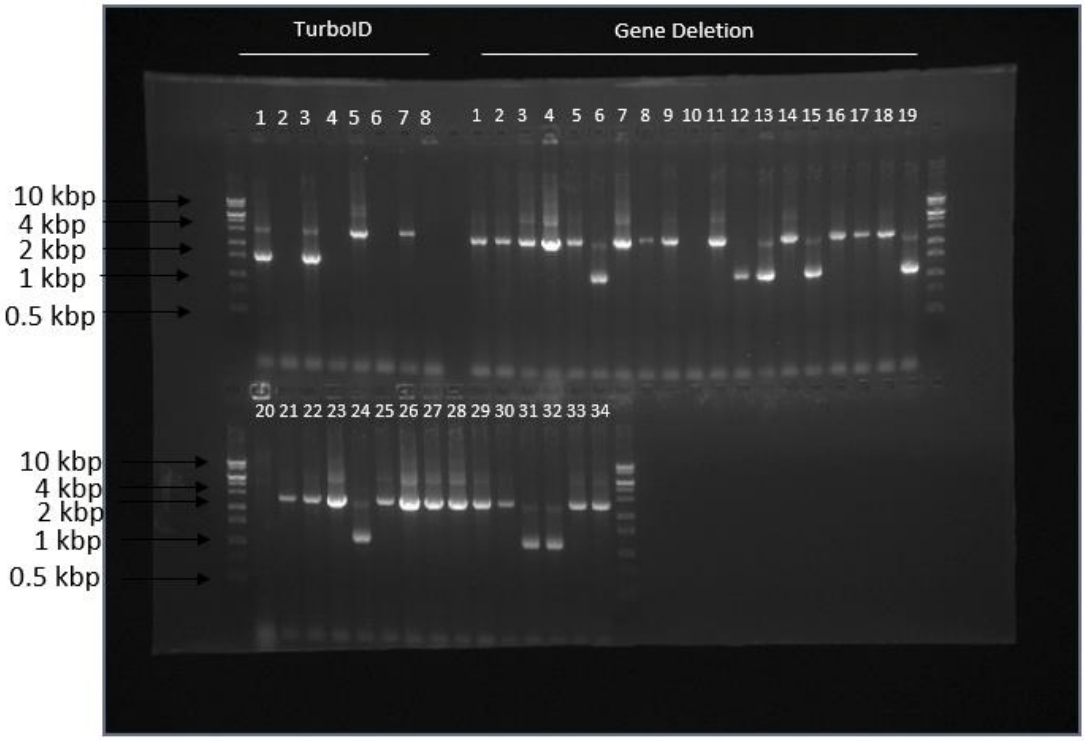

Figure 3.7

Figure 3.7: A gel exhibits that colony PCR was again used to assess the presence of the targeting sequeces into final vectors. The ligation product of final TurboID vector and 3' UTR-CDS SOE PCR product was transformed and screened, shown on the upper left of the gel. Eight TurboID colones in total grew on the antibiotic plate, of which two had bands at sizes that would indicate they were positive (2622 bp): colonies 5 and 7. The ligation product of the final gene deletion vector and the 3' UTR- 5'UTR SOE PCR product was transformed and screened, shown on the upper right and lower portion of the gel. Thirty four gene deletion colonies grew on the antibiotic plate. Numerous colonies expressed bands at 2622 bp indicating that they were positive for integration of the SOE product into the final vector.

With SOE PCR products integrated into destination vectors, wild type Py17XNL parasites were transfected, selected by pyrimethamine, and assessed for GFP expression by fluorescence microscopy as described in the Methods. Parasite populations were assessed by

genotyping PCR to detect the presence of transgenic parasites and to approximate the ratio of wild-type to transgenic parasites present. Genotyping PCR (gPCR) involved the use of three sets of primers: wild-type (WT), transgenic 3' (3' TG), and transgenic 5' (5' TG). Each of these primer sets would amplify a region in the genome of the parasites, selected such that amplification could confirm if the genome was transgenic. WT primer sets would amplify a portion of the wild-type Py17XNL genome; thus if a band was present at the appropriate size the parasites could be considered wild-type. 3' TG and 5' TG were both used to amplify regions spanning the site of integration; thus if bands were present with both at the appropriate sizes, the parasite could be considered transgenic. In reality, there was a mix of transgenic and wild type parasites in the group. Figure 3.8 exhibits the gPCR for PyTSN1::GFP and PyTSN1::TurboID::GFP. Flow cytometry had been used to sort the TSN1::GFP line, including both population 1 and population 2, with the ultimate goal of increasing the ratio of transgenic parasites to wild type parasites in a population. Figure 3.9 exhibits the gPCR for *pytsn1*$^{-}$,which necessitated using two wild-type primer sets, 3' WT and 5' WT. Three clones were used. Clone 1 was produced from the mice infected with 2.5 parasitized RBC/ 100 uL RPMI, and Clones 2 and 3 were produced from mice infected with 5 parasitized RBC/ 100 uL RPMI. The schematics in Figures 3.1-3.3 include designations of the location of the primers and the area amplified, and Appendix A includes the primers used. A plasmid positive control was run to ensure the transgenic primers were appropriate, and a wild-type control was run with Py17XNL to ensure the wild-type primers were appropriate and that the transgenic primers didn't amplify any off-target region.

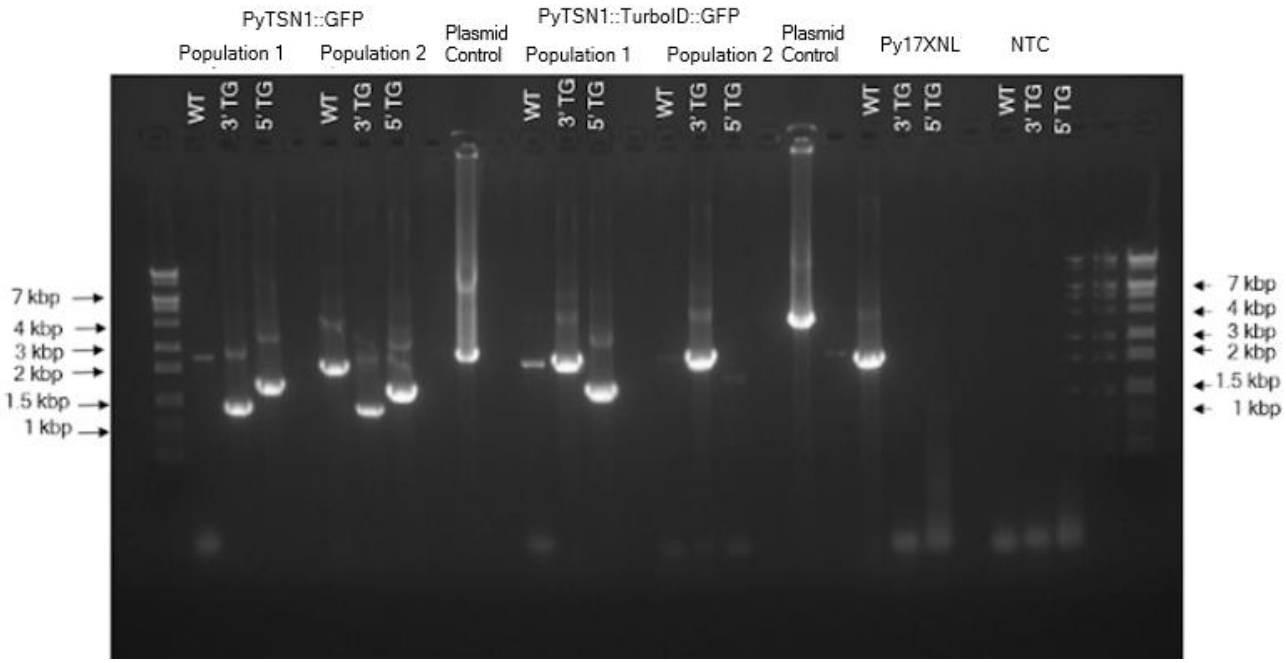

Figure 3.8

Figure 3.8: A gel of the genotyping PCR shows the presence of transgenic parasites of two lines: PyTSN1::GFP and PyTSN1::TurboID::GFP. Genotyping PCRs were conducted with three parasite lines: PyTSN1::GFP (see Figure 3.2), PyTSN1::TurboID::GFP (see Figure 3.1), and wild type Py17XNL as a control. Pairs of wild-type (WT) and transgenic (TG) primers were used to confirm that the plasmid DNA was integrated into the genomic locus as intended. The expected band sizes for the PyTSN1::GFP line included wild-type bands (visible with the WT primer set) at ~1800 bp and transgenic bands (visible with the TG primer set) of ~1367 bp for the 3' TG primers and ~1850 bp for the 5' TG primers. The plasmid positive control is the expected size of 2083 bp. The PyTSN1::TurboID::GFP line had expected band sizes of ~1800 bp for the WT primers to identify the presence of wild type parasites, and of ~1994 bp and ~1370 bp for the 3' TG primers and the 5' TG primers, respectively. The plasmid control had the expected size of 3049 bp. The Py17XNL wild type control exhibited only the band at ~1800 bp with WT primers, as expected. The plasmid positive control also behaved as expected for both lines. The No Template Control was conducted to ensure that no component of the PCR would produce a band sans template. Thus, the transgenic parasite lines used in this study were population 1 of the population 1 of the PyTSN1::GFP FACS line and PyTSN1::TurboID::GFP line.

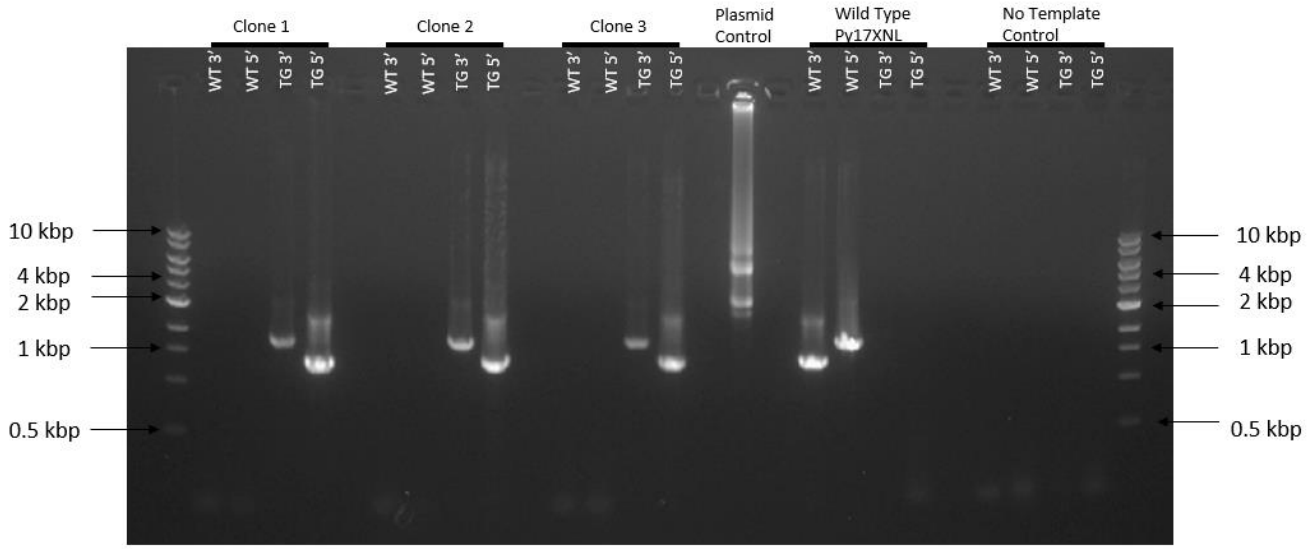

Figure 3.9

Figure 3.9: A gel of the genotyping PCR shows the presence of transgenic parasites of three clones of the *pytsn1*$^{-}$ parasite line. gPCRs were conducted with three parasites lines generated by limited dilution cloning. This gPCR confirms that all three clones are transgenic; all three exhibit no bands in the lanes including wild type primers, while they have bands of the appropriate size (TG 3'1367 bp, TG 5' 1747 bp) in lanes including transgenic primers. The relevant band for the TG 5' lane is not the brightest band, but the larger one. The plasmid control (2622 bp) and the wild type control (WT 3'1810 bp, WT 5' 1386 bp) were performed to ensure that the primers were working appropriately. The No Template control was performed to ensure PCR components did not amplify without a template present.

The size of the tagged protein product was analyzed by western blot to ensure that it was appropriate for a transgenic parasite (Figure 3.10). Whole parasite lysate from the respective parasite lines was probed with rabbit α-GFP primary antibody and anti-rabbit-conjugated HRP secondary antibody was applied to facilitate visualization. Recombinant GFP was also probed as a control, as the success of adding a C-terminal tag including GFP was being assessed by this blot. The PyTSN1::GFP line was approximately 148 kDa on the gel, indicating that it was likely the appropriate size and that the C-terminal tag was successful. The PyTSN1::TurboID::GFP line

also was approximately the appropriate size (183 kDa), indicating that the C-terminal tag was successful. The recombinant GFP control was the appropriate size (27 kDa).

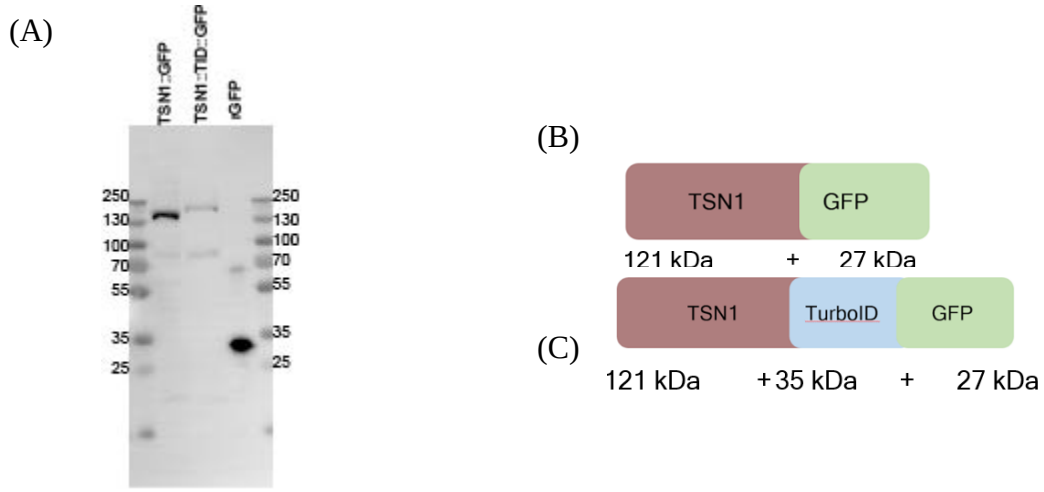

Figure 3.10

Figure 3.10: (A) A western blot exhibiting the size of proteins from the PyTSN1::GFP line and PyTSN1::TurboID::GFP line. Rabbit α-GFP primary antibody was used to bind GFP, and anti-rabbit-conjugated HRP secondary antibody was used to visualize. **(B) A schematic of the components of the modified protein include TSN1 and a GFP tag**, totaling a molecular weight of 148 kDa. **(C) A schematic of the components of the modified protein include TSN1, a TurboID tag, and a GFP tag**, totaling a molecular weight of 183 kDa.

The two PyTSN1:: GFP lines contained transgenic parasites, but population 1 contained fewer wild-type genomic loci than population 2 based on qualitative analysis of the gel. Population 1 of PyTSN1::TurboID::GFP was nearly entirely transgenic, however population 2 contained some wild-type parasites and the 5' transgenic primers did not successfully amplify a region of the genome. This may have been due to error in setting up the 5' TG gPCR. Limited dilution cloning produced three transgenic clones of the *pytsn1* gene deletion. The successful

deletion of *pytsn1* from the genome of parasites indicate that PyTSN1 is nonessential in asexual blood stage *P. yoelii* parasites.

The size of the protein produced by the transgenic clones can be seen in Figure 3.10 (B) and (C). The PyTSN1::GFP line was approximately the expected 148 kDa, and the PyTSN1::TID::GFP line was approximately the expected 183 kDa, confirming the tags were fused to the protein.

Immunofluorescence Assays

Transgenic parasites expressing PyTSN1 tagged with GFP were used to analyze PyTSN1 expression timing and localization in the asexual and sexual blood stage parasites. Immunofluorescence assays were conducted with mixed blood stage parasites using anti-GFPmut2 antibodies to detect PyTSN1::GFP. The stage of the parasite was determined by counterstaining with an appropriate stage-enriched protein (anti-PyACP for asexual blood stage parasites, anti- α tubulin for male gametocytes, and anti-PyCITH for gametocytes).

PyTSN1 in asexual blood stage parasites primarily localized to the cytoplasm of the parasite, though there were several instances of nuclear localization observed. This was consistent in stages of blood stage asexual development including trophozoites (Figure 3.11), and schizonts (Figure 3.12). Data on ring stage asexual blood stage parasites was not collected.

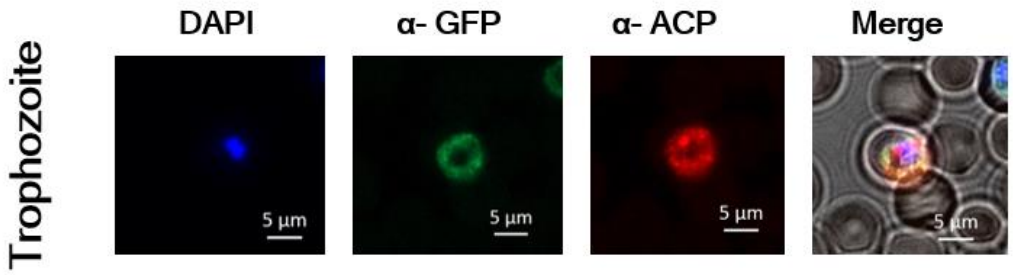

Figure 3.11

Figure 3.11: Cytosolic localization of PyTSN1 in trophozoites. Parasites prepared for immunofluorescence assay with anti-PyACP facilitated identification of asexual blood stage parasites. In these parasites, PyTSN1, marked by anti-GFP, presented in the cytoplasm in the majority of parasites, including trophozoite-stage parasites. Localization here is solely cytosolic. Scale bar is 5 microns.

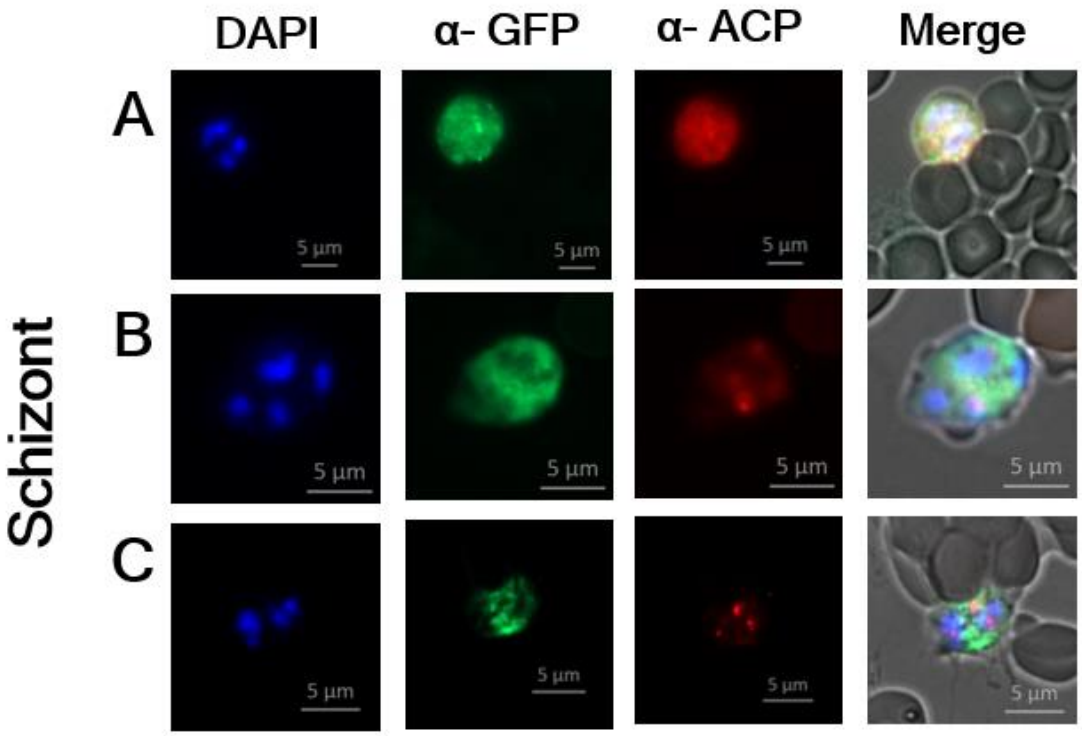

Figure 3.12

Figure 3.12: Cytosolic localization of PyTSN1 in schizonts. Parasites prepared for immunofluorescence assay with anti-PyACP facilitated identification of asexual blood stage parasites. In these parasites, PyTSN1, marked by anti-GFP, presented in the cytoplasm in the majority of parasites, as seen in (A) and (B). Some of the parasites exhibited nuclear adjacent localization, as seen in (C). Scale bar is 5 microns.

Female gametocytes had a consistent localization pattern as well, with PyTSN1 in the cytoplasm. In some cases, such as in Figure 3.13 (A) and (C), the localization was either in punctae or diffuse throughout the cytoplasm, but in each parasite PyTSN1 expression overlapped with its known binding partner PyCITH.

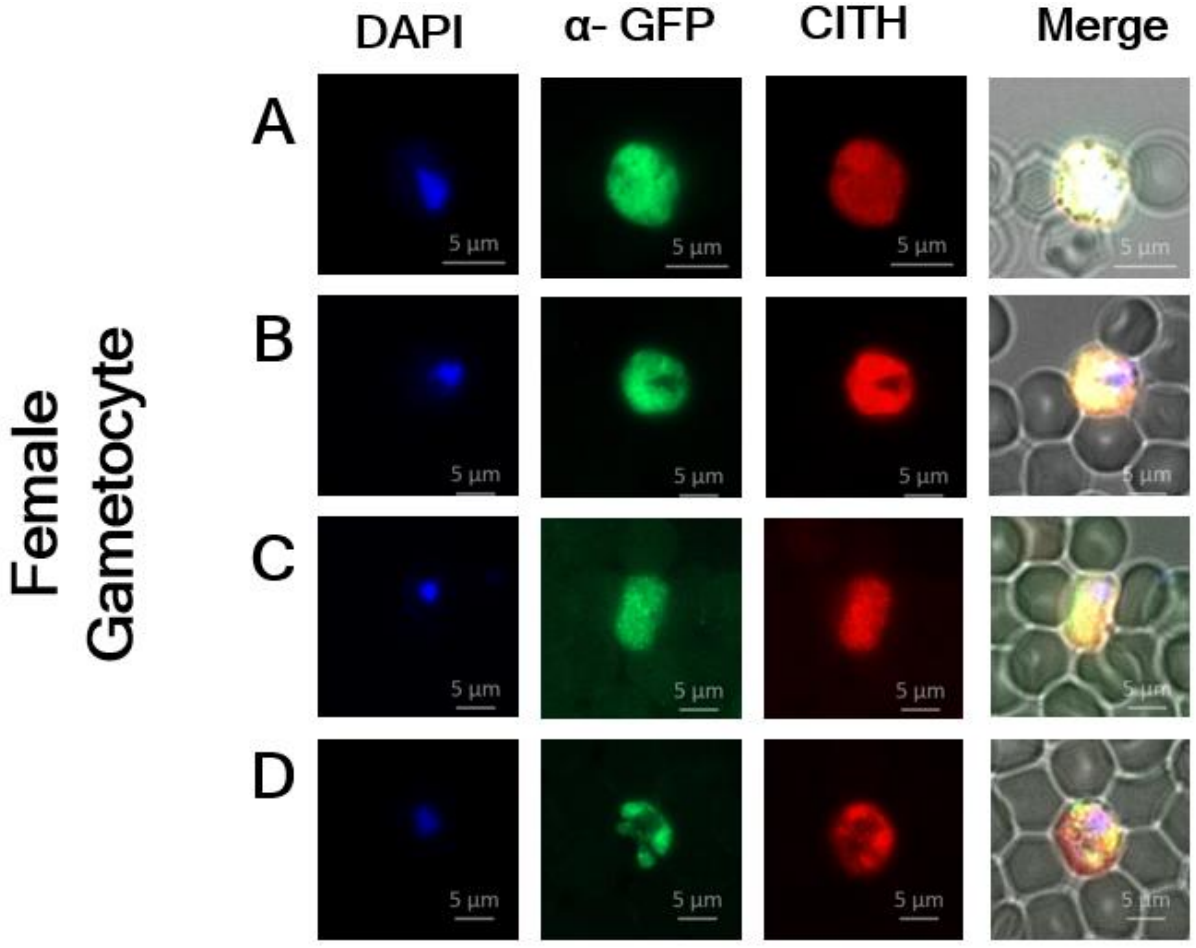

Figure 3.13

Figure 3.13: Cytoplasmic and granular localization of PyTSN1 in female gametocytes. Parasites prepared for immunofluorescence assay with strong anti-PyCITH signals were

identifiable as female gametocytes. Localization of PyTSN1 varied throughout female gametocytes, but primarily it was cytosolic. In some parasites, PyTSN1 localizes near the nucleus. Notably, PyTSN1 was found in puncta, in a localization pattern similar to PyCITH, an RNA binding protein associated with translation repression during sexual development.

Localization in male gametocytes was determined to be highly variable across individual parasites. PyTSN1 was visible in the nucleus, adjacent to the nucleus, in the cytoplasm and nucleus, and in the cytoplasm excluding the nucleus.

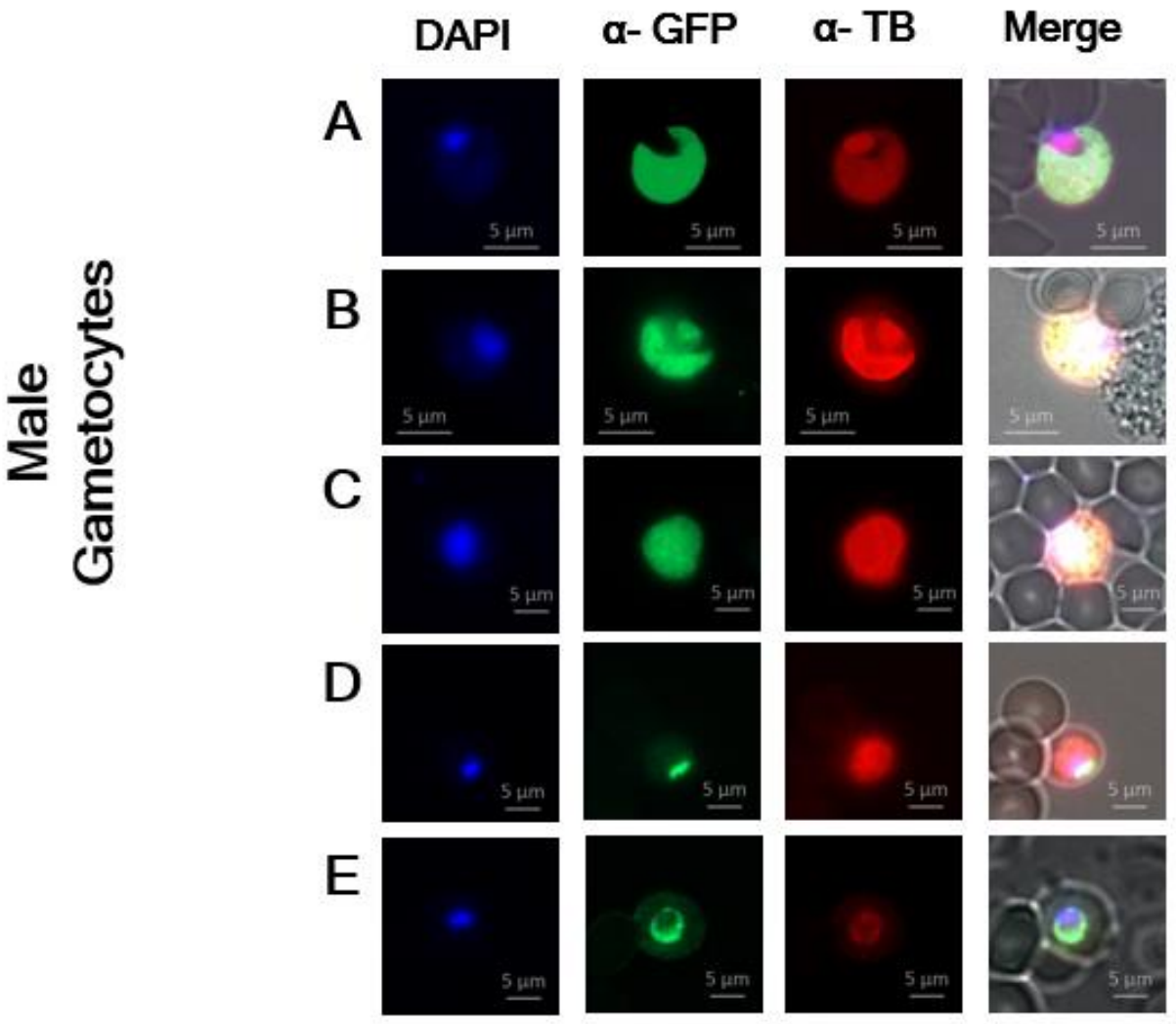

Figure 3.14

Figure 3.14: Mixed localization patterns for PyTSN1 in male gametocytes. Parasites prepared for immunofluorescence assay with a strong anti-α tubulin signal were identifiable as male gametocytes. Localization of PyTSN1 in male gametocytes varied greatly throughout all

IFAs. In some, including (C) and to a degree (B), localization was cytosolic. In others, including (D) and (E), localization was nuclear adjacent. In (B), it was observed that PyTSN1 localized to the nucleus in addition to the cytosol. In (A), localization was cytosolic and excluded the nucleus.

Proximity-Based Labelling

Empirical Determination of Biotin Supplementation Conditions

Proximity-based labeling experiments are useful to determine what proteins are in the near vicinity of the target protein in order to establish some tentative protein-protein interactions. If a protein is present significantly within the labeling radius, they may be interacting with the protein-of-interest. In the case of PyTSN1, its cellular function is uncharacterized; in order to understand what functions PyTSN1 may have, analyzing the proteins it is interacting with regularly at a particular stage gives an idea of what role it may play within the cell. BioID, *E. coli* BirA*, was the first proximity-based labeling tool considered for use in this project, however TurboID, BirA* that had undergone directed evolution[1] was determined to be a better fit due to its more promiscuous biotinylation capabilities and its shorter labeling time. TurboID biotinylates proteins within a ~10 nm radius of protein of interest when exogenous biotin is present, as exhibited in Figure 3.15.

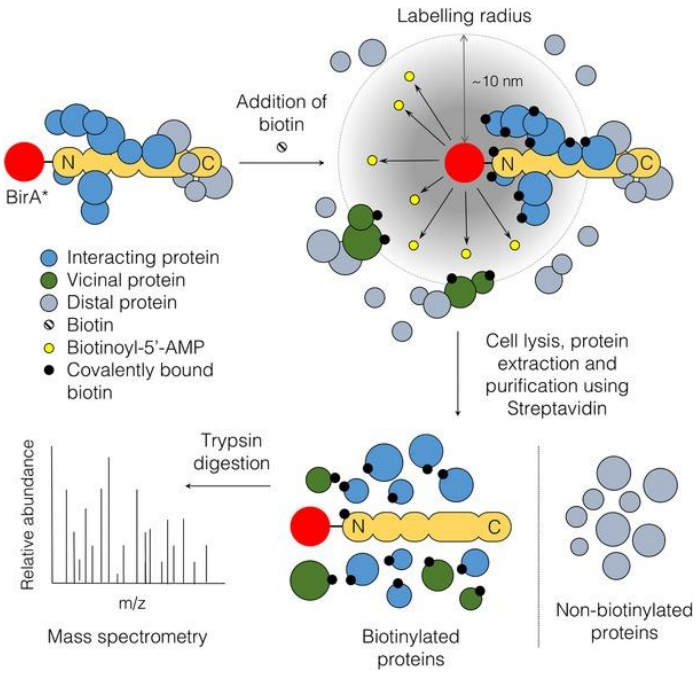

Figure 3.15

Figure 3.15: A schematic shows the workflow of a proximity-based labeling experiment with BioID. The experiment conducted for this thesis utilized TurboID, a modified form of BioID that had undergo directed evolution. Image from Varanite et al.

A control was used to label cytoplasmic proteins and establish a background of proteins common to the cytoplasm. The appropriate length of labelling time was determined in schizonts by supplementing with 150 uM biotin at various time points during *ex vivo* culture. Previous work done by Kelly Rios in the Lindner Lab has determined that 150 uM biotin is an appropriate concentration with which to supplement for BioID and TurboID experiments, as there is biotin naturally present in mouse blood (~4 ng / mL)[20] and in RPMI (~1uM). By supplementation, labelling with biotin is substantially increased and can enrich for proteins that interacted with PyTSN1 during the labeling window. Both the PyTSN1::TurboID::GFP and the unfused TurboID::GFP control were analyzed to determine appropriate labelling time. Ultimately, 4 hours labelling showed significant labelling, enough to be confident that it is not due to natural biotin. This experiment was conducted in schizonts.

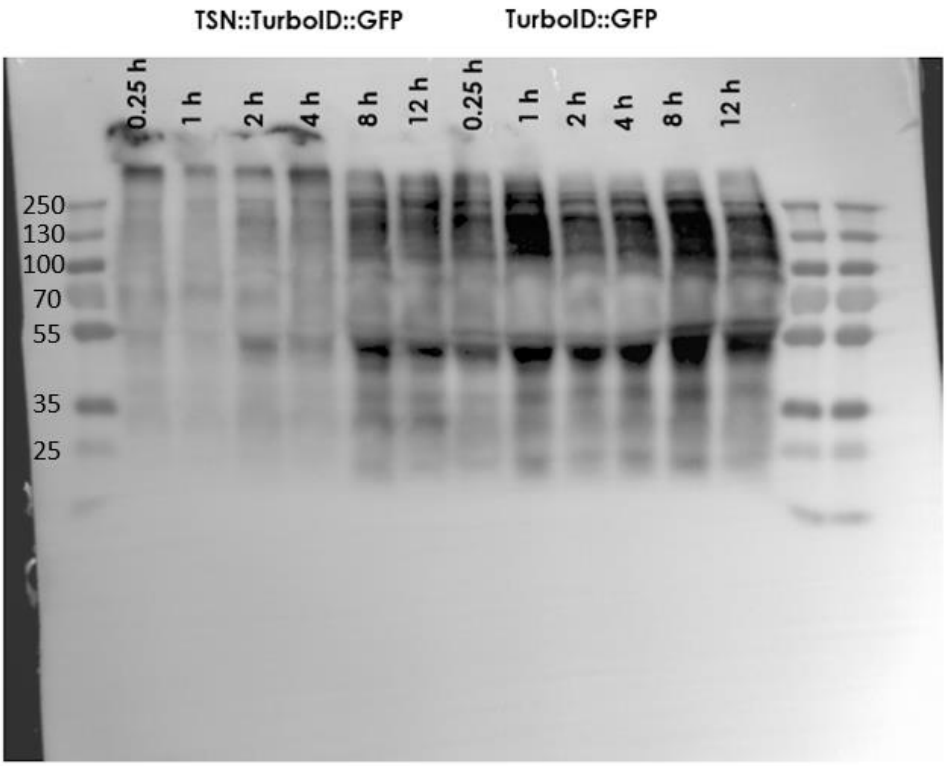

Figure 3.16

Figure 3.16: A western blot exhibiting all time points during determination of labeling time. Four hours labeling seemed an appropriate balance between ensuring labeling and not over-labeling. This image was taken at 2 seconds exposure time.

Capture of Biotinylated Proteins

After an appropriate duration of labelling with biotin was determined, magnetic streptavidin beads were utilized to capture biotinylated proteins. There is an exceptionally high-affinity noncovalent interaction between streptavidin, found on the beads, and biotin, which was covalently attached to the proteins labelled by the experiment ($K_d = 10^{-15}$M). Proteins were captured from both the PyTSN1::TurboID::GFP line and a control line containing unfused TurboID::GFP expressed with a strong constitutive promoter EF1α from a dispensable locus in the Py17XNL genome, *p230p*[4]. Before identification of captured biotinylated proteins by mass

spectroscopy, a quality control “pseudo-western blot” probing with streptavidin-HRP was conducted to ensure that the beads indeed bound the proteins of interest.

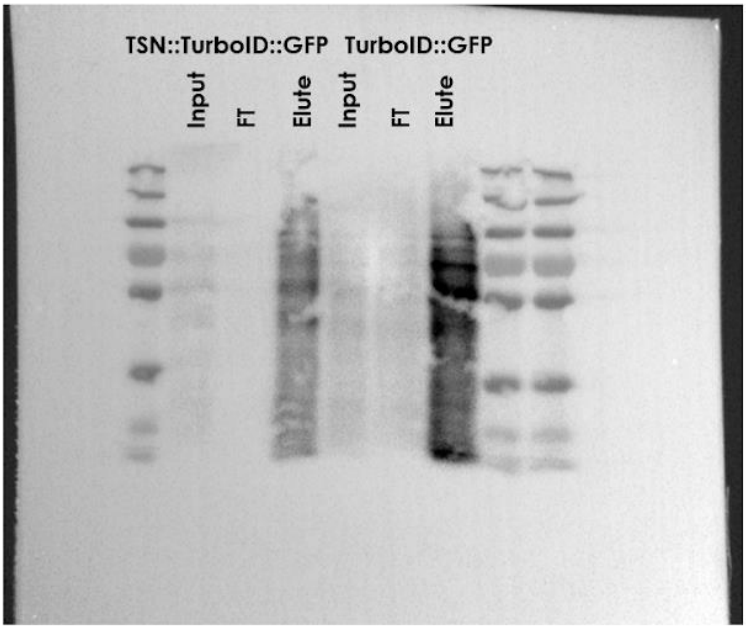

Figure 3.17

Figure 3.17: A quality control “pseudo-western blot” used to assess if the streptavidin beads had bound protein after labeling in schizonts. Protein was present in the elution of PyTSN1::TurboID::GFP, and there was litle present in the input or the flow-through, indicating that the protein had bound the beads. The TurboID::GFP line was the unfused control used. This also exhibited protein in the elution off of the beads and little in the input or flow-through. The remaining beads were sent to the Indiana Proteomics Core.

Mass Spectrometry Identification of Interacting Proteins

Samples that passed quality control experiments obtained were left on the streptavidin beads and sent to the Indiana Proteomics Core for on-bead, in solution tryptic digests and the resulting peptides were and run on a Thermo Scientific Q Exactive Plus Orbitrap LC-MS/MS System. The resulting data was analyzed by TPP. The experiments were conducted once in schizonts, which showed several proteins that were present in the experimental data in significant

numbers when compared to the control (Table 3.1) , and gametocytes, which showed only one significant protein present when compared to the control (Table 3.2).

With one replicate of data, definitive conclusions cannot be made. However, the presence of mRNA-interacting proteins in the dataset of proximal proteins to PyTSN1 in schizonts may indicate that PyTSN1 itself plays a role in mRNA-modulation. Putative polyadenylate-binding protein, a putative RNA helicase, putative mRNA decapping enzymes, and a putative eukaryotic translation initiation factor subunit all would indicate that in the vicinity of PyTSN1, mRNA is being modulated. Many of these proteins have also appeared in the DOZI/CITH/ALBA complex and the CAF1/CCR4/NOT complex, which may indicate PyTSN1's presence in these complexes. There were seventy-six proteins identified in the experimental PyTSN1::TurboID::GFP line that were not present in the unfused TurboID::GFP line. Among these unique proteins was PyTSN1, indicating that the data is valid as PyTSN1 has biotinylated itself, while it wasn't present in the background data. Unique proteins does not imply these are the only proteins with enriched labeling in the experimental line; of the 50% of proteins that were detected by both PyTSN1::TurboID::GFP, some may be enriched in the experimental over the unfused control.

Table 3.1: Biotinylated Proteins Identified by Mass Spectroscopy (Schizonts) Preliminary mass spectroscopy data shows a variety of putative proteins biotinylated over background by TurboID. These proteins are likely in the vicinity of PyTSN1 in schizonts. At the top of the list, as expected, is PyTSN1 which biotinylates itself over the course of the experiment.

Table 3.1

Gene ID	Protein Description	Experimental Independent Spectra	Control Independent Spectra
PY17X_0913800	tudor staphylococcal nuclease, (TSN1)	121	-
PY17X_1441700	polyadenylate-binding protein, putative (PABP)	23	14
PY17X_0504300	eukaryotic translation initiation factor subunit eIF2A, putative	15	5
PY17X_1429000	RNA helicase, putative	14	3
PY17X_0808800	heat shock protein 90, putative (HSP90)	15	9
PY17X_1035100	CUGBP Elav-like family member 2, putative (CELF2)	11	5
PY17X _1446600	T-complex protein 1 subunit gamma, putative (CCT3)	6	1
PY17X_0517000	mRNA-decapping enzyme subunit 1, putative (DCP1)	6	-
PY17X_1409100	mRNA-decapping enzyme 2, putative (DCP2)	6	-
PY17X_0707700	RNA binding protein, putative	4	-

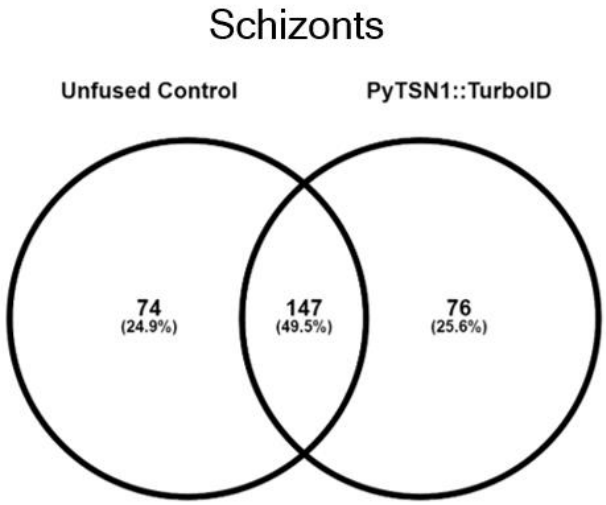

Figure 3.18

Figure 3.18: Venn Diagram of proteins detected by the unfused control (TurboID::GFP) and PyTSN1::TurboID::GFP during labeling of schizonts. Of the proteins detected, just under 50% were detected by both. Seventy-six unique proteins were detected by TurboID fused to PyTSN1. Diagram made with Venny.

TurboID experiments in gametocytes showed only one unique protein that appeared in the experimental with greater frequency than the control: PyTSN1. This would indicate that the experiment was functional, however the labelling of the unfused TurboID::GFP was much greater than that of the experimental TurboID fused to the target protein, PyTSN1. The cytosolic labelling of the TurboID::GFP control overwhelmed any labelling done specifically by the TurboID fused to PyTSN1. Thus, future work should explore shorter labeling times to determine if specific interactions can be observed over background generated by the unfused control. There were twelve unique proteins in the experimental PyTSN1::TurboID::GFP dataset, with 27.5% overlap of identified proteins between the experimental and control lines.

Table 2:Biotinylated Proteins Identified by Mass Spectroscopy (Gametocytes)
Preliminary mass spectroscopy data shows TSN1 was protein identified over background.

Table 3.2

Gene ID	Protein Description	Experimental Independent Spectra	Control Independent Spectra
PY17X_0913800	tudor staphylococcal nuclease, (TSN1)	152	5

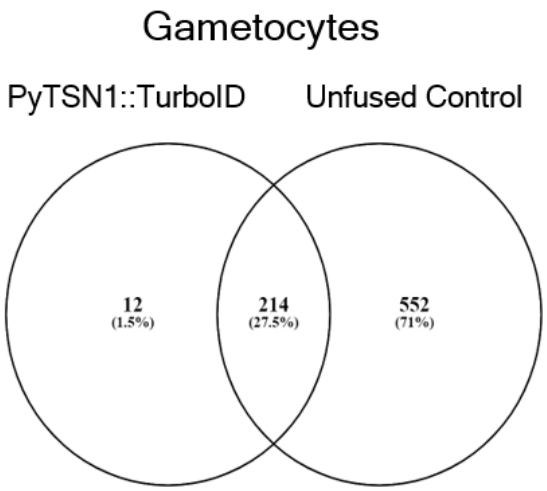

Figure 3.19

Figure 3.19 Venn Diagram of proteins detected by the unfused control (TurboID::GFP) and PyTSN1::TurboID::GFP during labeling of gametocytes. Of the proteins detected, 27.5% were detected by both lines. Twelve unique proteins were detected by TurboID fused to PyTSN1. Diagram made with Venny.

Phenotype Analysis

A preliminary experiment was run to analyze the phenotype of *pytsn1*$^{-}$ parasites, however numbers were not recorded, thus the experiment was considered failed. Centers of movement were counted prior to, and the centers of movement for the *pytsn1*$^{-}$ parasite line were lower than

that of the control parasite line expressing GFP. The feed proceeded anyway, and oocysts were counted on mosquito midguts at day 10 post feed. The numbers of mosquitoes with GFP expressed on the midgut was lower in the experimental *pytsn1*$^{-}$ line in comparison to the control line. The number of oocysts on an infected midgut was also lower in the experimental *pytsn1*$^{-}$ line in comparison to the control line. On day 14, mosquito salivary glands were dissected and salivary gland sporozoites counted by hemocytometer. The experimental *pytsn1*$^{-}$ line had no countable salivary gland sporozoites.

Chapter 4

Discussion

In my independent honors research, I have studied the previously uncharacterized Tudor Staphylococcal Nuclease 1 (TSN1) protein in the rodent malaria parasite *Plasmodium yoelii.* TSN1 associates with known translational repression complexes that are critical to parasite transmission, but its role in these processes is unknown. Through reverse genetics approaches, I have generated three transgenic parasite lines, and I investigated PyTSN1's importance, expression timing, and localization, and I identified proximal proteins to PyTSN1.

A major challenging component to reverse genetics studies with malaria parasites is simply the generation of critical reagents, such as the plasmids needed to create the desired transgenic lines. Figure 3.4 and many other gels not included exhibited the difficulty of amplifying the 5' UTR region of the PyTSN1 gene. Initially, it was assumed that there was a problem with experimental conditions, and the Tm of the PCR run was varied by -/+ 5 C. However, when that failed to produce an amplified region, the primers were examined. It was determined that the 5' reverse primer (Appendix A) was the complement of the intended sequence. A new primer was developed (Appendix A) and used, but still no amplification was visible. A member of the Lindner Lab, Dr. Kevin Hart eventually succeeded in amplifying the 5' UTR of TSN1 by utilizing a previously developed primer (Appendix A) in lieu of the 5' UTR Reverse primer that had been designed. With the amplification of the 5' UTR, the SOE PCR of the 3' UTR (previously amplified, visible in Figure 3.4) and the 5' UTR could proceed. This facilitated the development of the plasmid required for the gene deletion parasite line.

While the gene deletion line was not successfully used to examine a phenotype in the life cycle due to time constraints, the very fact that it could be generated shows that PyTSN1 is nonessential to blood stage parasites. This is consistent with what has been shown the putative TSN in *Plasmodium berghei* and TSN in *P. falciparum,* both designated as dispensable for blood stage parasites in largescale genetic screens[27, 6] . The preliminary experiment done to analyze the phenotype of the gene deletion did not provide any usable data, however the results may indicate the deletion of *pytsn1* results in impaired transmission. Data from full phenotyping experiments would be useful in confirming this. The idea that transmission will be impaired through a gene deletion raised questions as to PyTSN1's role in transmission. For this reason, proximity-based labeling experiments were conducted with gametocytes in addition to schizonts.

The PyTSN1::GFP line was used in the immunofluorescence assays to determine expression timing and localization. PyTSN1 was shown to localize to the cytoplasm in asexual blood stage parasites, female gametocytes, and some male gametocytes. In asexual blood stages trophozoites and schizonts, cytosolic and nuclear-adjacent localization was clear, though there was a minor presence in the nucleus in some parasites (Figures 3.11 and 3.12). Ring-stage parasites were not analyzed. Female gametocytes exhibited primarily cytosolic localization, excluded from the nucleus in some parasites but with low fluorescence in the nucleus of others. Notable in female gametocytes as well was localization into cytosolic puncta, with a localization pattern similar to that of PyCITH and other granule proteins. (Figure 3.15) Localization varied among male gametocytes, with PyTSN1 found exclusively in the cytoplasm, overlapping with the nucleus, and surrounding the nucleus. (Figure 3.14)

Of interest in these data is the primarily cytoplasmic localization, as this contradicts the assumptions one may make when comparing to other protozoan parasites. In *Entamoeba*

histolytica, another protozoan parasite, a TSN-like protein has been identified which binds upstream regulatory elements in the genome. As its likely function is a transcription factor, this protein typically exhibits nuclear localization. This protein is TSN-like and not a member of the TSN family; it has 36% similarity and contains five Staphylococcal Nuclease domains and one Tudor motif. This difference in protein composition may account for differences in function[2]. However, this functionality as a transcription factor during the asexual lifecycle and development of gametocytes may be more unlikely for *Plasmodium yoelii,* as though PyTSN1 was observed in the nucleus in some parasites, this localization pattern was inconsistent.

Additionally, when immunofluorescence assays were conducted on *Plasmodium falciparum* in previous studies, it was shown that in asexual blood stage parasites PfTSN colocalized for the most part with DAPI in the parasite's nucleus, with low amounts of the protein visible via fluorescence in the cytoplasm[11]. PyTSN1 and PfTSN are orthologous and share structural homology as determined by a blast search through PlasmoDB. Why these two proteins that were suggested to be highly similar have vastly different localization patterns may simply be due to the use of a rodent model, however differences may also be due to the methods used in analyzing PfTSN. One conclusion Hossain and Sunil came to was that PfTSN was an essential protein in blood stage parasites. It is not, as confirmed by PlasmoDB. It is possible that similar erroneous conclusions were made in regard to PfTSN localization or function. Nuclear adjacent and cytoplasmic localization in schizonts, as illustrated by Figure 3.12, was the predominant pattern in *P. yoelii.*

Female gametocyte localization was of interest in particular due to the observed granules in some female parasites as observed by IFA. While not all PyTSN1 localized to puncta; this is reminiscent of the expression pattern of DOZI and CITH proteins with a combination of granular

and cytosolic diffuse expression. Granules containing CITH and DOZI are functioning as translational repressors, associated with other proteins integral for RNA processing in preparation for a transmission event[12]. Some of these granules appear to overlap in the immunofluorescence images, however the density of the granules differs between PyTSN1 and PyCITH, as seen in Figure 3.13. While PyTSN1 is most dense along the left most side of the cell, PyCITH granules are most dense in the central part of the cell. It is possible that PyTSN1 is colocalized with PyCITH, which is in turn in a complex with DOZI and other vital translational repressors in female gametocytes, as they have remarkably similar localization patterns. Proximity-based labelling data in gametocytes would be helpful in elucidating this pattern of localization, as it would show if PyTSN1 is in proximity to (and likely interacting with) critical granule components such as PyCITH and DOZI.

It was surprising to see that there was such variation in localization patterns in male gametocytes, seen in Figure 3.14. Some exhibited solely cytoplasmic localization, without a trace of significant fluorescence in the nucleus, while others shows localization in the nucleus and near the nucleus in a small area. In some parasites, TSN1 localization was dispersed throughout the cell, including the nucleus. Colocalization with α-tubulin in a crescent shape around the far side of the cell and in the nucleus itself can be seen in one image, while another shows solely a nuclear adjacent localization. Little can be concluded from this information alone. Phenotyping data of the *pytsn1*- parasites may provide more clues as to the importance of this protein to male gametocytes and gametes.

PyTSN1 was tagged with a variant of *E. coli* BirA* enzyme (TurboID) to allow for proximal protein interactions to be identified. Among the proteins that PyTSN1 was in close proximity (~10 nm) in schizonts with were a number of RNA-interacting proteins, including

polyadenylate binding protein (PABP), eukaryotic translation initiation factor subunit 2A (eIF2A), a putative RNA helicase, and two subunits of a putative mRNA-decapping enzyme (DCP1, DCP2) (Table 3.1). Labelling in gametocytes identified only one protein in proximity to the TurboID enzyme: PyTSN1 itself (Table 3.2).

In the one replicate of available data for asexual parasites, PyTSN1 was shown to interact with a variety of proteins, notably those involved with RNA processing in various ways. This is consistent with the function of TSN family proteins interacting with RNA. In *P. falciparum,* PfTSN inhibition causes reduced numbers of specific mRNAs, indicating that PfTSN is required to facilitate the survival of particular mRNAs[23]. My data linking PyTSN1 to PABP, a putative RNA helicase, and mRNA decapping enzymes support this to an extent. In *P. yoelii,* PABPs are involved in RNA metabolism and translational repression[14], and functions by binding the poly-A tail of transcripts where it can facilitate trafficking of the transcript, protect from premature degradation, or participate in nonsense-mediated decay. mRNA decapping enzymes remove the 5' cap from a transcript, which is required to maintain stability. A transcript without a cap is quickly degraded. While the presence of PABP may indicate mRNA is being protected from degradation, the proximity of mRNA decapping enzymes would indicate the contrary. As PABP is present on cellular mRNAs that are not being degraded, and as ALBA4, which I hypothesize is interacting with PyTSN1, functions to regulate normal mRNA turnover in schizonts, it is likely that PyTSN1 is playing a role involved in mRNA decay in schizonts. That being said, it is not unheard of for proteins to hold dual roles within the same stage of the parasite life cycle; PyTSN1 may be protecting certain mRNAs. The data does not make its role clear. My data also shows proximity between PyTSN1 and eIF2A, a translation initiation factor, indicating that it does play some role in modulating translation of transcripts. Additionally, PfTSN has been

shown to rely on its nuclease domain to ensure the process of moderating which mRNAs survive to be translated, indicating that it is not just binding RNA but also cleaving it[11]. Neither proximity-based labelling nor localization studies can confirm or refute the hypothesis that PyTSN1 depends on its nuclease domains to degrade mRNAs in the cell as a method of moderating translation.

One of the reasons TSN1 was a protein of interest was due to its appearance in immunoprecipitation pull-downs of proteins interacting with ALBA4 and CCR4 in schizonts. Notably lacking in the one replicate of asexual blood stage proximity-based labelling data is ALBA4, which plays a major role in post-transcriptional regulation in asexual stage parasites as well as gametocytes, and the members of the CAF1/CCR4/NOT complex, which likely plays a role in mRNA regulation in asexual and sexual blood stages. ALBA4 localizes to the cytosol in asexual blood stage parasites. In rings, it is adjacent to the nucleus, in trophozoites it is diffuse in the cytoplasm, and in schizonts it is found in punctate foci. While the localization pattern of PyTSN1 matched that of ALBA4 in trophozoites, PyTSN1 was not localized to puncta in schizonts[15]. Observation of PyTSN1 in immunoprecipitation data[15] inspired this line of research, and not seeing ALBA4 in this data set may indicate that while TSN1 may be involved in ALBA4-mediated RNA processing, TSN1 may also be functioning in processes without ALBA4. The lack of ALBA4 in the dataset may also be due to a lack of proximity; ALBA4 and PyTSN1 may be interacting outside of the range of TurboID (~10 nm). Additionally, this was only one replicate of data. Subsequent replicates may show ALBA4 as one of the proximal proteins to PyTSN1.

The data collected by proximity-based labelling in gametocytes makes it difficult to draw concrete conclusions regarding the function of PyTSN1 in transmission events. An initial study

was run on gametocytes, as seen in Table 2. These data are valid, as indicated by the significant labelling of the target protein, TSN1, over the background provided by the control. However, this is the only protein that was biotinylated to a significant degree. This is perhaps an issue where the experimental line with TurboID conjugated to PyTSN1 was more lowly expressed than the free TurboID produced by the control; if that is the case, the background is too high for data to be visible over it. A potential solution to this problem would be to generate a parasite line containing TurboID under a promoter with similar activity to that of the promoter governing TSN1. Additionally, labelling time could be reduced to one hours in lieu of four hours, which could reduce overlabeling in the control. The latter can be tried readily, as it does not require production of a new transgenic parasite line.

Even without complete replicates of proximity-based labelling data, one general conclusion can be drawn: PyTSN1 likely plays a role in regulating mRNAs post-transcriptionally. In asexual blood stages, it is in the vicinity of primarily proteins that interact with mRNA. In female gametocytes, its presence in granules is indicative that it may be involved in translational repression. Further studies would be needed in order to better elucidate the function of PyTSN1.

Obtaining more optimal proximity-based labelling data for gametocytes and repeating the experiment for asexual blood stage parasites is a top priority for follow-up projects investigating PyTSN1. These data would clarify what is known about TSN1's interactions in asexual blood stage parasites (including confirming a proximal interaction with ALBA4) and would elucidate what TSN1 is interacting with in gametocytes. In particular, it would be important to determine whether TSN1 interacts proximally with CCR4, CITH, and DOZI. CCR4 seen in gametocytes would be reciprocal data for previous studies and would also confirm that TSN1 is involved in

moderation of transcripts in male gametocytes. In the case of CITH and DOZI, the presence or lack of this data would confirm TSN1's localization or possible location within translational repression granules in female gametocytes. Additionally, crosslinking immunoprecipitation data from gametocytes would be useful in identifying proteins associating with TSN1 via long-range interactions.

Confirming or refuting the hypothesis that PyTSN1 is involved in regulation of post-transcriptional or translational processes would only be the first step, however. If TSN1 is indeed involved in moderating transcripts, several questions arise, namely

1) how is TSN1 moderating these transcripts

2) how does TSN1 work in tandem with other proteins to achieve the intended moderation

3) which transcripts does TSN1 aide in modulating

4) what is the effect on the parasite if TSN1 is absent

The last question would perhaps be the easiest to address with the current experimental set up. A gene deletion parasite line has already been generated, cloned, and is readily available to be used to infect mice and run through the life cycle. While this was attempted, data points were lost and thus the experiment was considered failed. The general result, however, would indicate that there may be a transmission phenotype. Completion of this experiment would provide valuable insight into what becomes dysregulated when TSN1 is no longer functional. As previous work has shown PfTSN impairment affects normal parasite development, analysis of the phenotype of *pytsn1* deletion would be interesting data. Experiments related to this will be continued in the Lindner lab; undergraduate student Taylor Dickson is planning on analyzing the effect of *pytsn1* gene deletion on centers of movement by injecting a defined number of parasites

into a mouse and counting both centers of movement and parasitemia daily. This will show if there is a defect in male gametocyte activation or if the gene deletion affects the asexual blood stage lifecycle in some way.

RNA-immunoprecipitation RNA-seq could be conducted to identify the particular transcripts that PyTSN1 directly interacts with, using the already generated parasite line PyTSN1::GFP and anti-GFP antibody-coated beads. Similarly, comparative RNA-seq techniques could be used to analyze transcript quantity in both wild-type and *pytsn1*$^{-}$ parasites in a relevant life cycle stage, thus identifying which transcripts are dysregulated, addressing the third question and supplementing known information about the phenotype of the gene deletion. This method would provide interesting data if done in asexual blood stage parasites and in gametocytes.

The first and second questions are related to the mechanisms of TSN1's function. Micrococcal nuclease inhibitors could be used to impede function of the nuclease domains of TSN1, and the result could be observed. This experiment could be conducted with existing parasite line PyTSN1::GFP. If transcripts become dysregulated, the nuclease domains would be considered vital for the function of the protein, perhaps indicating that PyTSN1 is functioning in a similar way to PfTSN. After determining what transcripts PyTSN1 interacts with (if it does interact with transcripts), the transcripts could be compared to find common sequences that would perhaps function as a method by which PyTSN1 recognizes the transcripts. Other possibilities include recognition by secondary structure, which could be potentially be analyzed by Structure-Seq.

Tudor staphylococcal nuclease proteins are found throughout the domains of life and provide essential functions for many organisms. *Plasmodium spp.* may also rely on these proteins to develop through their lifecycle and successfully transmit between host and vector.

Further work to elucidate the role that PyTSN1 actually plays is required, however I am hoping the research described here is a starting point for those who wish to do so.

Appendix A: Primers

Primer	SEL Primer Designation	Sequence
PyTSN1 3' UTR Amplification Forward	25-72	ccggtaccGTAATTTCTATTTCCTAATCCCC TTATCTTCGGAATATCG
PyTSN1 3' UTR Amplification Reverse	25-73	gggcccagctagcATGAGCCTGATAAGGAACC TGCACCTACTGAAGAAACC
PyTSN1 CDS Amplification Forward	25-70	GCTCATgctagctgggcccCGAAAACAATCTAA TAAGTGGAGATAAAGCAAAACTCTCTG
PyTSN1 CDS Amplification Reverse	25-71	ggactagtTGCATAATTGTCATCGTAATTTAT GTCTCCATAAGACCATATGCC
PyTSN1 5' UTR Amplification Forward	25-74	GCTCATgctagctgggcccGGTAATTTGTTTACT AACCATTAGGGAATATAAATATAGCC
PyTSN1 5' UTR Amplification Reverse	25-10	CGGATATAACCTGCTTTACTACACCGACG AGTCTTTCC
PyTSN1 gPCR 3' WT Forward gPCR 5' TG Forward	26-80	GCAAAGAGCAGTGCAAATATGTATTATCAC ATGTG
PyTSN1 -gPCR 3' WT Reverse -gPCR 3' TG Reverse -gPCR 3' TG Reverse (deletion)	26-81	GCTAACACCCACAATAATTCCTCTATTGATA AATGGCTACC
PyTSN1 -gPCR plasmid Reverse -gPCR plasmid Reverse (deletion) -gPCR 5' TG Reverse -gPCR 5' TG Reverse (deletion)	10-51	CATCACCATCTAATTCAACAAGAATTGGGAC AACTCCAGTGAAAAGTTCTTCTCCTTTAC
PyTSN1 -gPCR plasmid Forward -gPCR plasmid Forward (deletion) -gPCR 3' TG Forward	13-61	CCAGGAGGAGAAAGGCATTAAGTACAAA TTTGAAGTATATGAGAAG

-gPCR 3’ TG Forward (deletion)		
PyTSN1 -gPCR 5’ WT Forward (deletion) -gPCR 5’ TG Forward (deletion)	27-14	GAGGCCAGCGGGGTCGACTAGGCG
PyTSN1 -gPCR 5’ WT Reverse (deletion)	27-15	CTCTTACATAAGGGTACACATTTGAGAAT GGCTTCTC

Bibliography

1. Branon T.C., Bosch J.A., Sanchez A.D., Udeshi N.D., Svinkina T., Carr S.A., Feldman J.L., Perrimon N., Ting A.Y. (2017) Efficient proximity labeling in living cells and organisms with TurboID. *Letters to Nature Biotechnology*

2. Calixto-Galves M., Romero-Diaz M., Garcia-Munjoz A., Salas-Casas A., Pais-Morales J., Galvan I.J., Rodriguez M. A. (2011) Identification of a polypeptide containing Tudor and staphylococcal nuclease-like domains as the sequence-specific binding protein to the upstream regulatory element 1 of *Entamoeba histolytica. International Journal for Parasitology 41,* 775-782

3. Cazares-Apatiga J., Medina-Gomez C., Chaves-Munguia B., Calixto-Galvez M., Orozco E., Vasquez-Calzada C., Martinez-Higuera A., Rodriguez M.A. (2017) The Tudor Staphylococcal Nuclease Protein of *Entamoeba histolytica* Participates in Transcription Regulation and Stress Response. *Frontiers in Cellular and Infection Microbiology 7,* 52

4. Cowman A.F., Healer J., Marapana D., Marsh K. (2016) Malaria: Biology and Disease. *Cell* 167:610-624

5. Dijk, M. R., van Schaijk B.C.L., Khan S.M., van Dooren M.W., Ramesar J., Kaczanowski S., van Gemert G.J.(2010) Three Members of the 6-Cys Protein Family of Plasmodium Play a Role in Gamete Fertility. *PLoS Pathogens* 6,

6. Gomes A.R., Bushell E., Schwach F., Girling G., Anar B., Quail M.A., Herd C., Pfander C., Mordrzynska K., Rayner J.C., Billker O. (2015) A genome-scale vector resource enables high-throughput reverse genetic screening in a malaria parasite. *Cell Host & Microbe 17,* 404-413

7. Guerreiro A., Deligaianni E., Sanots J.M., Silva P.A.C.G., Louis C., Pain A., Janse C.J., Franke-Fayard B., Carret C.K., Siden-Kiamos I., Mair G.R. (2014) Genome-wide RIP-Chip analysis of translational repressor-bound mRNAs in the *Plasmodium* gametocyte. *Genome Biology 15,* 493

8. Gutierrez-Beltran E., Denisenko T.V., Zhivotovsky B., Bozhov P.V. (2016) Tudor staphylococcal nuclease: biochemistry and functions. *Cell Death and Differentiation 23,* 1739-1748

9. Gutierrex-Beltran E., Elander P.H., Dalman K., Crespo J.L., Moschou P.N., Uversky V.N., Bozhkov P.V. (2020) Tudor Staphylococcal Nuclease acts as a docking platform for stress granule components in *Arabidopsis thaliana. bioRxiv preprint.*

10. Hart K.J., Oberstaller J., Walker M.P., Minns A.M., Kennedy M.F., Padykula I., Adams J.H., Lindner S.E. (2019) *Plasmodium* male gametocyte development and transmission

are critically regulated by the two putative deadenylases of the CAF1/CCR4/NOT complex. *PLoS Pathogens, 51(1)*

11. Hossain M.J., Korde R., Singh S., Mohmmed A., Dasaradhi P.V.N., Chauhan V.S., Malhotra P. (2007) Tudor domain protiens in protozoan parasites and characterization of *Plasmodium falciparum* tudor staphylococcal nuclease. *International Journal for Parasitology 38,* 513-526

12. Mair, G. R., Lasonder E., Garver L. S., Franke-Fayard B. M. D., Carret C. K., Weigant J. C. A. G., Dirks R. W, Dimopoulos G., Janse C. J., Waters A. P. (2010) Universal Features of Post-Transcriptional Gene Regulation Are Critical for *Plasmodium* Zygote Development. *PLoS Pathogens 6, e1000767*

13. Mair G.R., Braks J.A.M., Garver L.S., Wiegant J.C.A.G., Hall N., Dirks R.W., Khan S.M., Dimopolous G., Janse C.J., Waters A.P. (2006) Regulation of Sexual Development of *Plasmodium* by Translational Repression. *Science 313,* 667-669

14. Minns A.M., Hart K.J., Subramanian S., Hafenstein S., Lindner S.E. (2020) Nuclear, Cytosolic, and Surface-Localized Poly(A)-Binding Proteins of *Plasmodium yoelii. mSphere 3, e00435-17*

15. Munoz E.E., Hart K.J., Walker M.P., Kennedy M.F, Shipley M.M., Lindner S.E. (2017) ALBA4 modulates its stage-specific interactions and specific mRNA fates during *Plasmodium* growth and transmission. *Molecular Microbiology 106(2),* 266-284

16. Lasonder E., Rijpma S.R., van Schaijk B.C.L., Hoeijmakers W.A.M., Kenshce P.R., Gresnigt M.S., Italiaander A., Vos M.W., Woestenenk R., Bousema T., Mair G.R., Khan S.M., Janse C.J., Bartfai R., Sauerwein R.W. (2016) Integrated transcriptomic and proteomic analyses of *P. falciparum* gametocytes: molecular insight into sex-specific processes and translation repression. *Nucleic Acids Research 44,* 6087-6101

17. Reddy B.P.N., Shrestha S., Hart K.J., Liang X., Kemirembe K., Cui L., Lindner S.E. (2015) A bioinformatic survey of RNA-binding proteins in *Plasmodium. BioMed Central Genomics 16,* 890

18. Rios K.T., Lindner S.E. (2019) Protein-RNA interactions important for *Plasmodium* transmission. *PLoS Pathogen 15(12)*

19. Roux K.J., Kim D.I., Raida M., Burke B. (2012) A promiscuous biotin ligase fusion protein identifies proximal and interacting proteins in mammalian cells. *The Journal of Cell Biology* 196:801-810

20. Rusckowski M., Fogarasi M., Fritz B., Hnatowich D.J. (1997) Effect of endogenous biotin on applications of streptavidin and biotin in mice. *Nuclear Medicine and Biology 24,* 263-268

21. Sengupta M.S., Boag P.R. (2012) Germ Granules and the Control of mRNA Translation. *Life 64,* 586-594

22. Snow R.W. Omumbo J.A. (2006) Malaria. In Jamison D.T. et al (eds). *Disease and Mortality in Subsaharan Africa* 2nd edition. pp. 195-214. World Bank, Washington DC

23. Sunil S., Hossain M.J., Ramasamy G., Malhotra P. (2008) Transient silencing of *Plasmodium falciparum* Tudor Staphylococcal Nuclease suggests an essential role for the protein. *Biochemical and Biophysical Research Communications 372,* 373

24. Varnaite, R.; MacNeill, S.A. (2016) Mapping local protein interactomes by proximity-dependent labeling with BioID. *Proteomics* 19

25. World Health Organization. (2019) World Malaria Report 2019.

26. Wrinkler G.S., Balacco D.L. (2013) Heterogeneity and complexity within the nuclease module of the CCR4-Not complex. *Frontiers in Genetics* 4, 296

27. Zhang M., Wang C., Otto T.D., Oberstaller J., Liao X., Adapa S.R., Udenze K., Bronner I. F., Cassandra D., Mayho M., Brown J., Li S., Swanson J., Rayner J. C., Jiang R. H. Y., Adams J. H. (2018) Uncovering the essential genes of the human malaria parasite *Plasmodium falciparum* by saturation mutagenesis. *Science 360,* eaap7847

Academic Vita

OLIVIA SMITH
oms5081@psu.edu

EDUCATION

The Pennsylvania State University **2020**
Major: Bachelor of Science in Microbiology
Thesis: "*Characterization of Plasmodium yoelii Tudor Staphylococcal Nuclease, PyTSN1"*

AWARDS

Schreyer Honors College Scholar **2016-Present**
Dean's List (6x) **2016-Present**
Eberly College of Science Undergraduate Research Grant **2018, 2019**
Top Scholar Award, Pathobiology Program, University of Washington
University of Washington Provost Scholarship for Academic Excellence

TEACHING EXPERIENCE

Guided Study Group Leader, Penn State Learning, The Pennsylvania State University

8/2017 – 12/2019

I lead weekly group study sessions and taught students to problem solve in a variety of Math courses, including Calculus I, Calculus II, and Finite Mathematics.

RESEARCH

Lindner Lab, The Pennsylvania State University

1/2018 – Present

In the Lindner Laboratory as an independent undergraduate researcher, I have focused on the rodent malaria parasite *Plasmodium yoelii.* I have specifically focused upon the protein PyTSN1, a previously uncharacterized protein associated with translational repressors. I have presented this research at the Penn State Undergraduate Exhibition (2018 and 2019) and at the Out in STEM National Conference in Detroit, MI (2019).

National Science Foundation Research Experience for Undergraduates, Black Hills State University

6/2019 –8/2019

I worked with a multidisciplinary team to conduct research at the Sanford Underground Research Facility (SURF), specifically investigating deep underground microbial diversity by sequencing and analyzing communities in the waters of SURF. I presented this research at the South Dakota Established Program to Stimulate Competitive Research Symposium.

ADDITIONAL SKILLS

- Knowledge of basic laboratory skills associated with organic chemistry, culturing microbes, and generating recombinant DNA
- Experience creating transgenic organisms via transfection
- Ability to isolate, purify and characterize protein via column chromatography, dialysis, centrifugation, crystallization, etc.
- Experience with various types of mouse surgeries such as tail snips, tail-vein injections, and cardiac punctures
- Familiarity with performing immunofluorescence assays and using fluorescence microscopy
- Experience with *Anopheles* mosquito midgut and salivary gland dissections
- Experience with Illumina Next Generation Sequencing